Geo 892 – 001: Biophysical Models and Applications in Ecosystem Analysis

Feb. 22, 2024

5:00 pm – 7:50 pm; GEO 120

Jan 22: Introduction & Biophysical Essentials for Ecosystem Models

Update from Jan 21, 2024

FAO ET model and reference ET_o: https://www.youtube.com/watch?v=gtV_RpXsMJI

Introduction: Concept, History, Type, Development and Variety of ecosystem models

Video: How Wolves Change Rivers in Yellowstone National Park

Video: Moose-wolve interactions at the Isle Royal National Park

Lecture 1: Micrometeorological Essentials (temperature, moisture, radiation, wind, energy balance, turbulences, eddy-covariance method)

Handout: Unit and unit conversions for carbon, water and energy

Reading: Chapter 1

Exercise 1: Radiation Distributions across Terrestrial Ecosystems (Solar.PY).

Update

Class Webpage for files and schedule: http://lees.geo.msu.edu/courses/geo892-2024/

Potential journals: J of American Water Resources Association; Hydrological Processes, Land; Agronomy; Journal of Water Processes; IJWRD; Nature Climate Change;

Dr. Gang Dong is interested in being a co-author of this manuscript.

Demonstration of processing EC data by Dr. Gang Dong: download EddyPro 7 | Software Downloads (licor.com); Data will be shared through class webpage Jan. 5

FAO ET model and reference ET_o: https://www.youtube.com/watch?v=gtV_RpXsMJI

Ecosystem Models: What? Why?

- Abstractions of real-world system or process

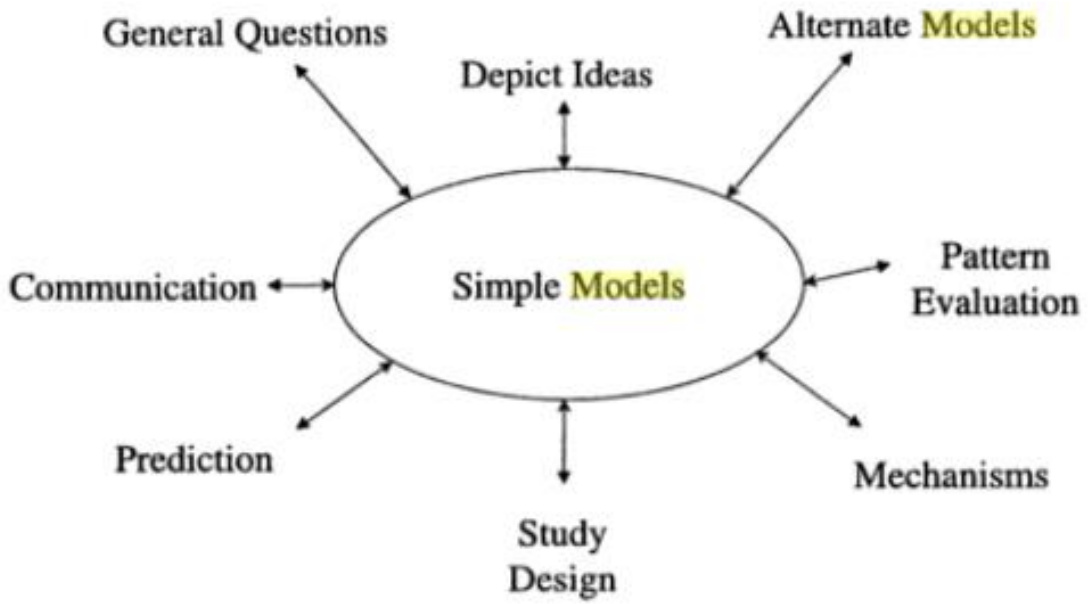

Figure 4.5. The utility of simple models in ecosystem science. The connections suggest that simple models can be effective tools toward progress in the various areas of research depicted.

Canham, C. D. W., Cole, J., & Lauenroth, W. K. (2003). *Models in ecosystem science*. Princeton University Press.

Biogeochemical Cycles of Terrestrial Ecosystems: Carbon, Water, Nutrient, and Energy in Terrestrial Ecosystems

1) What is ecosystem ecology?
2) What are the major components of ecosystem analysis?
3) Cycles of carbon and water
4) Energy balance
5) Global Warming Potentials (GWP)

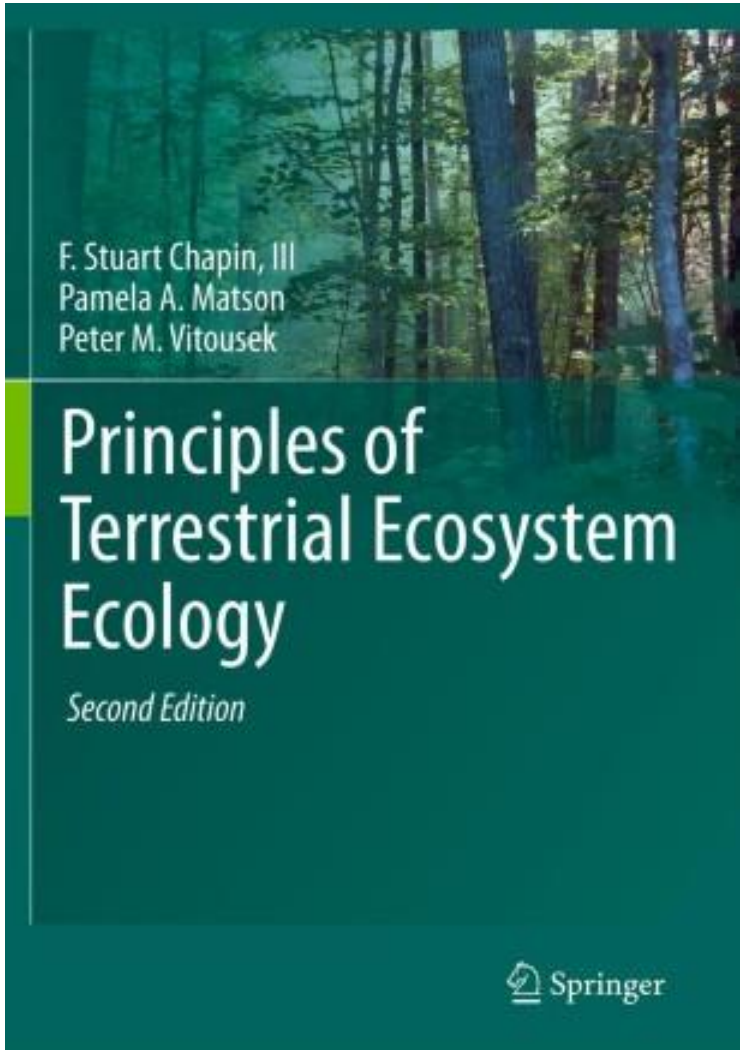

References

1) Chapin III, F. S., Matson, P. A., & Vitousek, P. (2011). *Principles of terrestrial ecosystem ecology*. Springer Science & Business Media.
2) Waring, R. H., & Schlesinger, W. H. (1985). Forest ecosystems. *Analysis at multiples scales*, 55.
3) Ågren, G. I., & Andersson, F. O. (2011). *Terrestrial ecosystem ecology: principles and applications*. Cambridge University Press.
4) Schlesinger, W. H. (Ed.). (2005). *Biogeochemistry* (Vol. 8). Elsevier.
5) Perry, D. A. (1994). *Forest ecosystems*. JHU Press.

What is “Ecosystem Ecology”?

- Ecosystem components are cohesively connected through various processes and interactions!
- Quantify and model these interactions through computer models have been a key elements of ecosystem analysis

Example: **How Wolves Change Rivers**

https://www.youtube.com/watch?v=ysa5OBhXz-Q

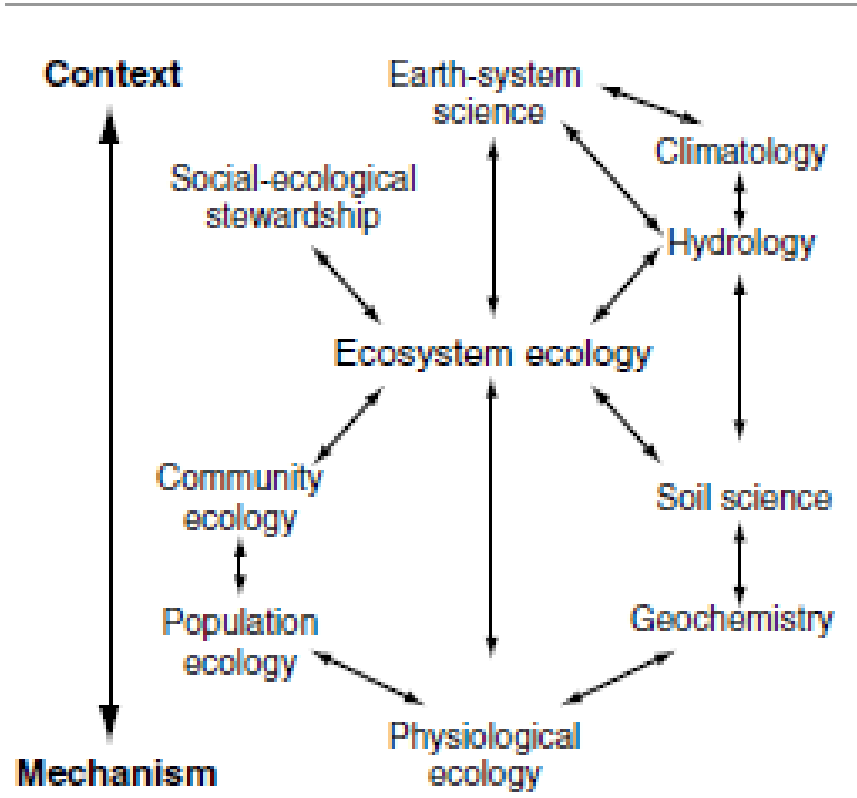

Fig. 1.3 Relationships between ecosystem ecology and other disciplines. Ecosystem ecology integrates the principles of several biological and physical disciplines, determines the resources available to society, and provides the mechanistic basis for Earth-System science

The story is about the mechanisms, suggesting that a model should also focus on the underlying processes.

Forest Ecosystems (Waring & Running 2007)

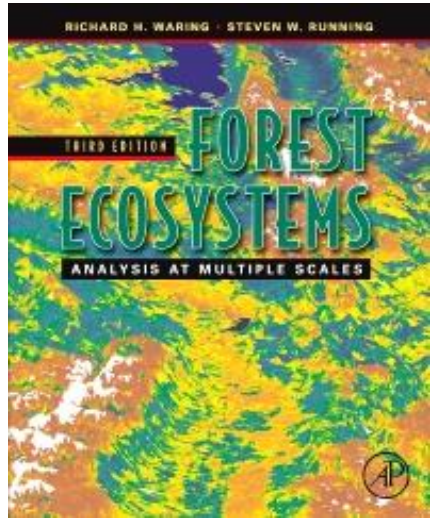

1. Forest Ecosystem Analysis at Multiple Time and Space Scales
2. Water Cycles
3. Carbon Cycle
4. Mineral Cycles
5. Temporal Changes in Forest Structure and Function
6. Susceptibility and Response of Forests to Disturbance
7. Spatial Scaling Methods for Landscape and Regional Ecosystem Analysis
8. Regional and Landscape Ecological Analysis
9. The Role of Forests in Global Ecology
10. Advances in Eddy-Flux Analyses, Remote Sensing, and Evidence of Climate Change

https://www.google.com/books/edition/Forest_Ecosystems/6YjhssXQ2AUC?hl=en&gbpv=1&pg=PA20&printsec=frontcover

In sum,

1 The Ecosystem Concept
2 Earth's Climate System
3 Geology, Soils, and Sediments
4 Water and Energy Balance
5 Carbon Inputs to Ecosystems
6 Plant Carbon Budgets
7 Decomposition and Ecosystem Carbon Budgets
8 Plant Nutrient Use
9 Nutrient Cycling
10 Trophic Dynamics
11 Species Effects on Ecosystem Processes
12 Temporal Dynamics
13 Landscape Heterogeneity and Ecosystem Dynamics
14 Changes in the Earth System
15 Managing and Sustaining Ecosystems

Joshua M. Epstein (2008), *Journal of Artificial Societies and Social Simulation* 11(4 12); Http://jasss.soc.surrey.ac.uk/11/4/12.html

1) Explain (very distinct from predict)
2) Guide data collection
3) Illuminate core dynamics
4) Suggest dynamical analogies
5) Discover new questions
6) Promote a scientific habit of mind
7) Bound (bracket) outcomes to plausible ranges
8) Illuminate core uncertainties.
9) Offer crisis options in near-real time
10) Demonstrate tradeoffs / suggest efficiencies
11) Challenge the robustness of prevailing theory through perturbations
12) Expose prevailing wisdom as incompatible with available data
13) Train practitioners
14) Discipline the policy dialogue
15) Educate the general public
16) Reveal the apparently simple (complex) to be complex (simple)

Epstein, J. M. (2008). Why model?. *Journal of Artificial Societies and Social Simulation*, *11*(4), 12.

Pre-computer Era models

- Look up tables
- Simple empirical relationships

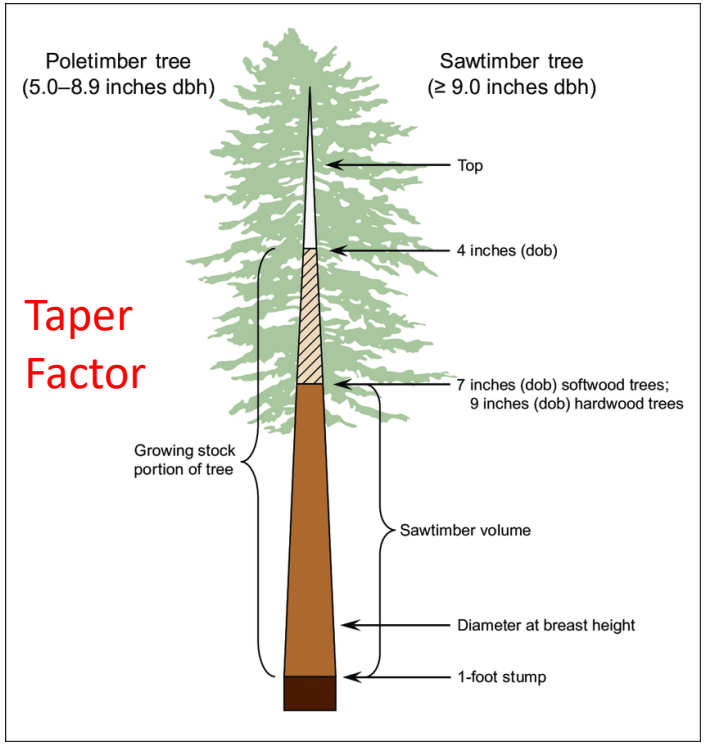

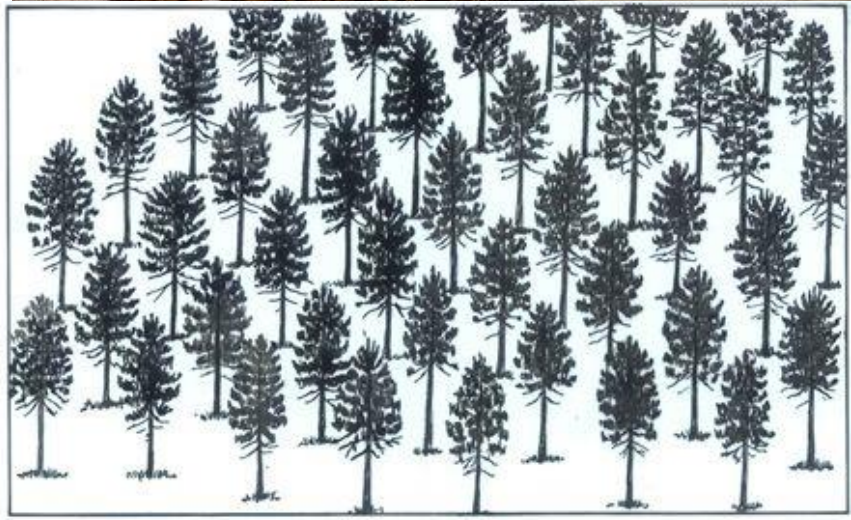

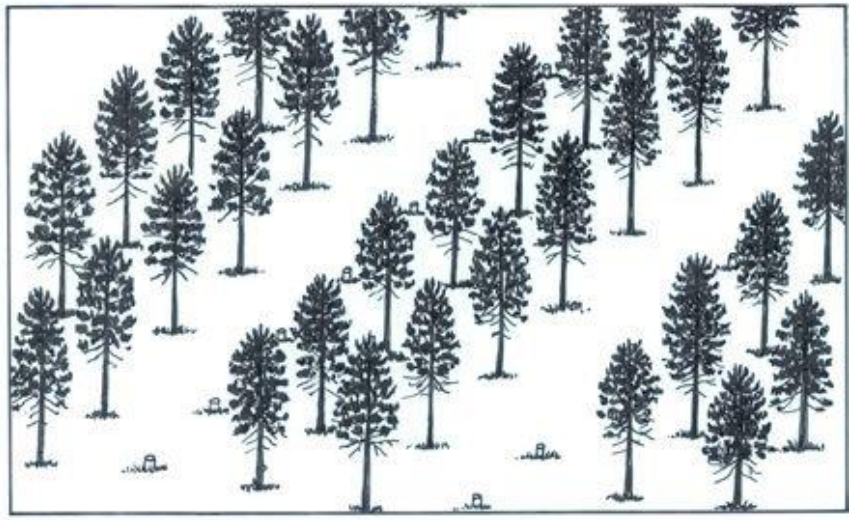

A tree

Volume$= \alpha \cdot DBH^{\beta}$

Volume$= \alpha \cdot Height \cdot DBH^{\beta}$

A forest

Volume$= \alpha \cdot [Height \cdot DBH^{\beta}] \cdot Density$

Volume$= \alpha \cdot [Height \cdot DBH^{\beta}] \cdot Density \mid Site\ Index|Species$

Volume$= \alpha \cdot [Height \cdot DBH^{\beta}] \cdot Density \mid Site\ Index|Species|management$

Biomass = Volume · Wood Density

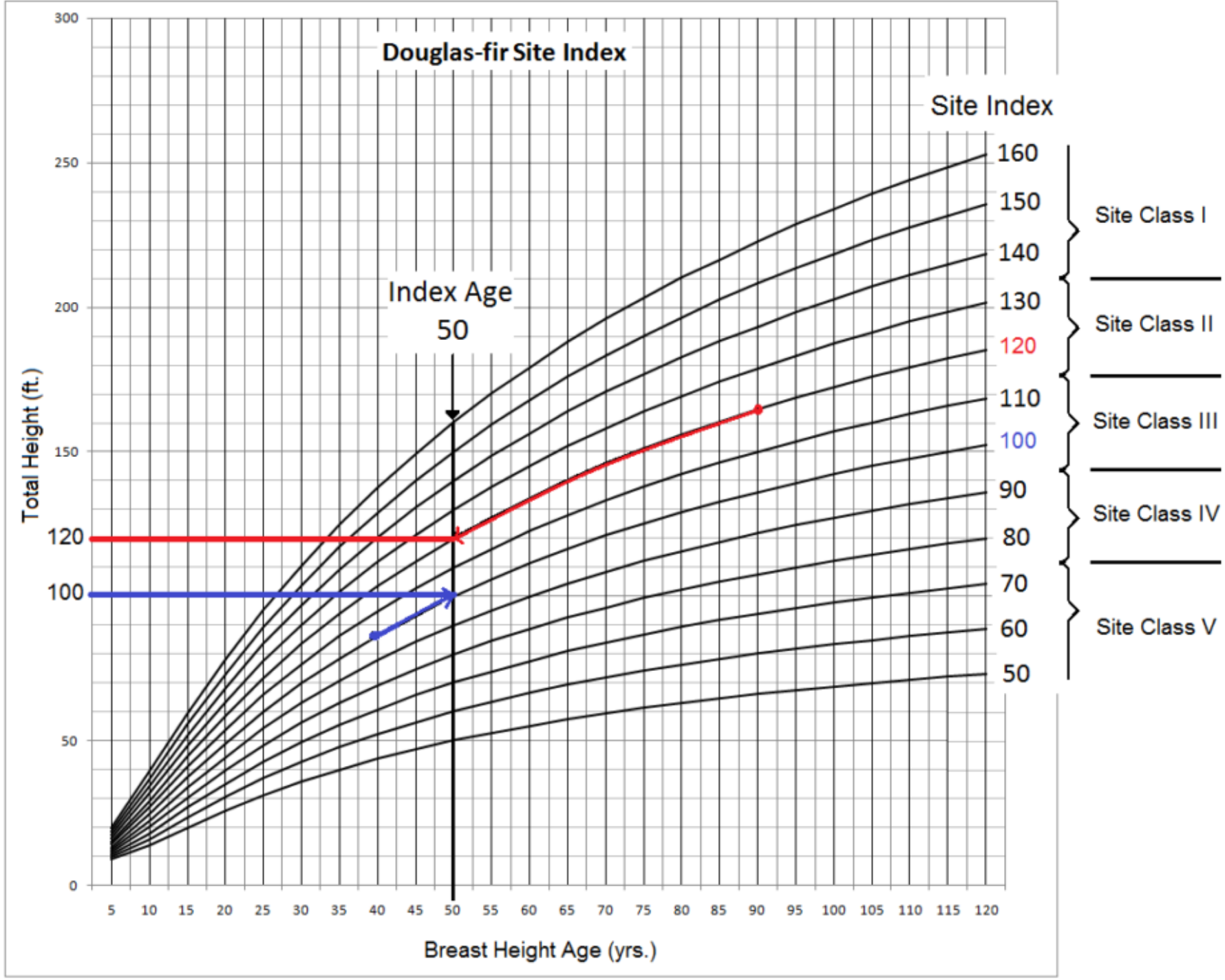
Douglas-fir Site Index
Site Index
Index Age
50
Total Height (ft.)
Breast Height Age (yrs.)
300
250
200
150
120
100
50
0
5 10 15 20 25 30 35 40 45 50 55 60 65 70 75 80 85 90 95 100 105 110 115 120
160
150
140
130
120
110
100
90
80
70
60
50
Site Class I
Site Class II
Site Class III
Site Class IV
Site Class V

Computer Era models

- Increasing the number of variables
- Mostly based on empirical relationships
- Climatic, soil, disturbances, management as regulators
- Interactions among components (e.g., species, soil-plants) are considered
- Example: JOBAWA, FORET models (a.k.a. GAP models)

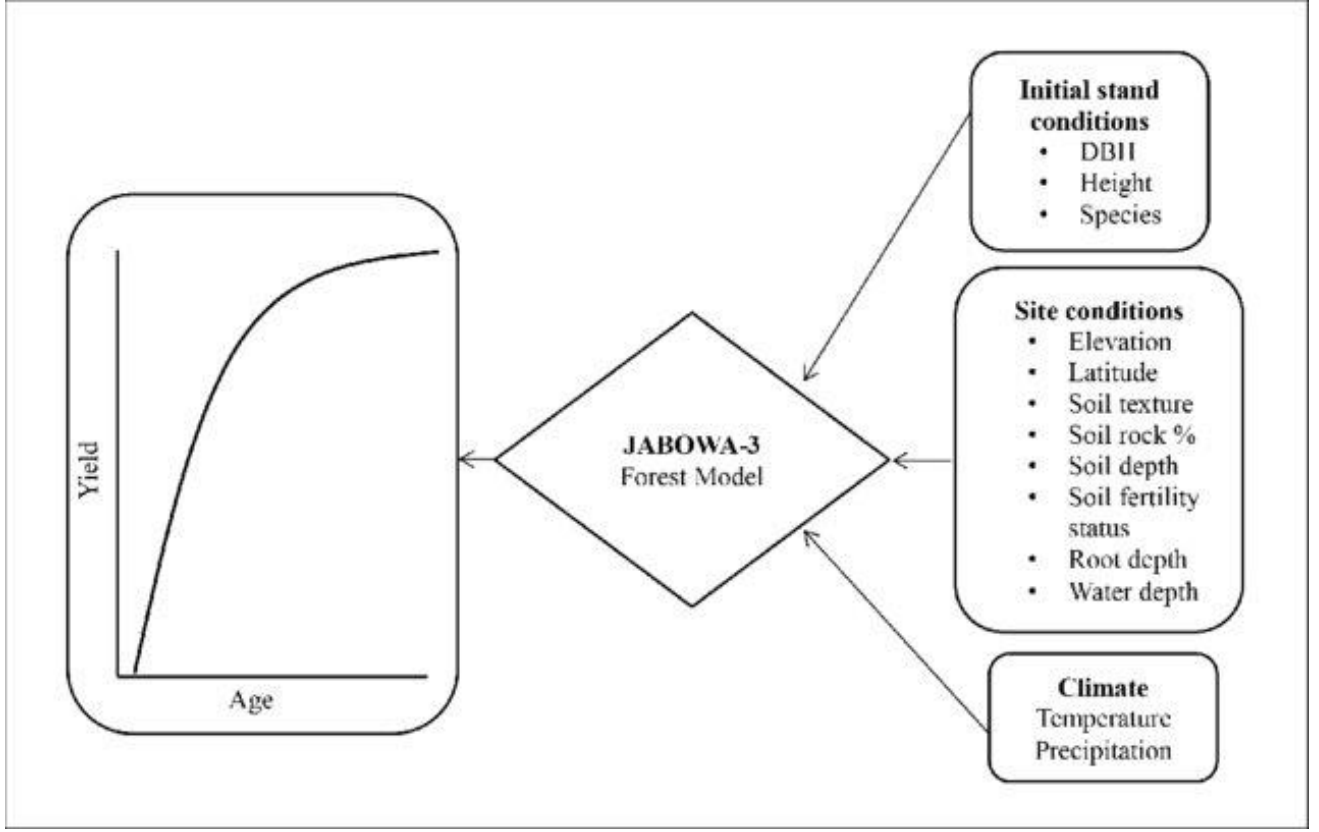

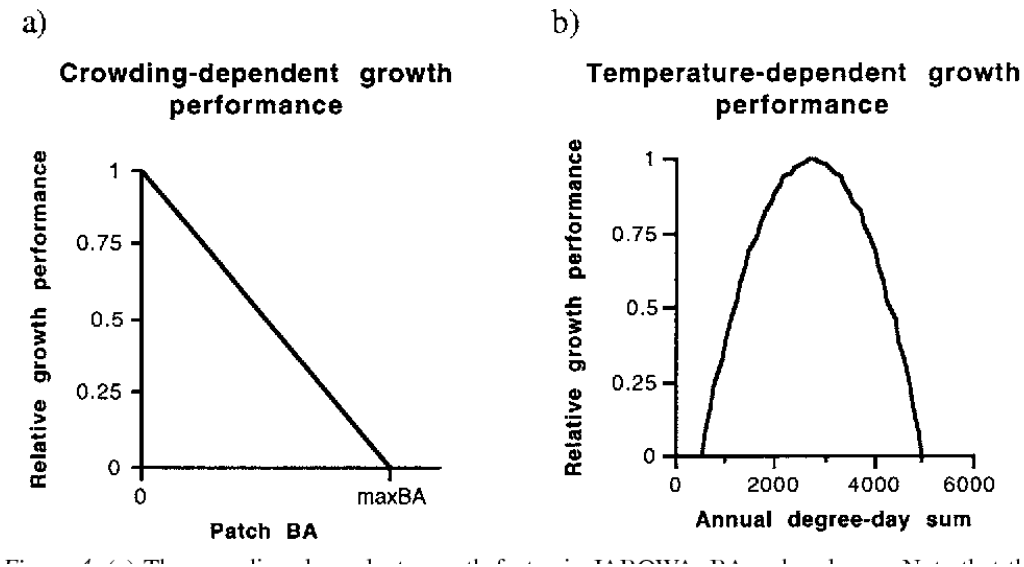

Ashraf, M. I., Bourque, C. P. A., MacLean, D. A., Erdle, T., & Meng, F. R. (2012). Using JABOWA-3 for forest growth and yield predictions under diverse forest conditions of Nova Scotia, Canada. *The Forestry Chronicle*, *88*(6), 708-721.

Individual-based models (IBMs) of complex systems emerged in the 1960s and early 1970s, across diverse disciplines from astronomy to zoology. Ecological IBMs arose with seemingly independent origins out of the tradition of understanding the ecosystems dynamics of ecosystems from a 'bottom-up' accounting of the interactions of the parts. Individual trees are principal among the parts of forests. Because these models are computationally demanding, they have prospered as the power of digital computers has increased exponentially over the decades following the 1970s.

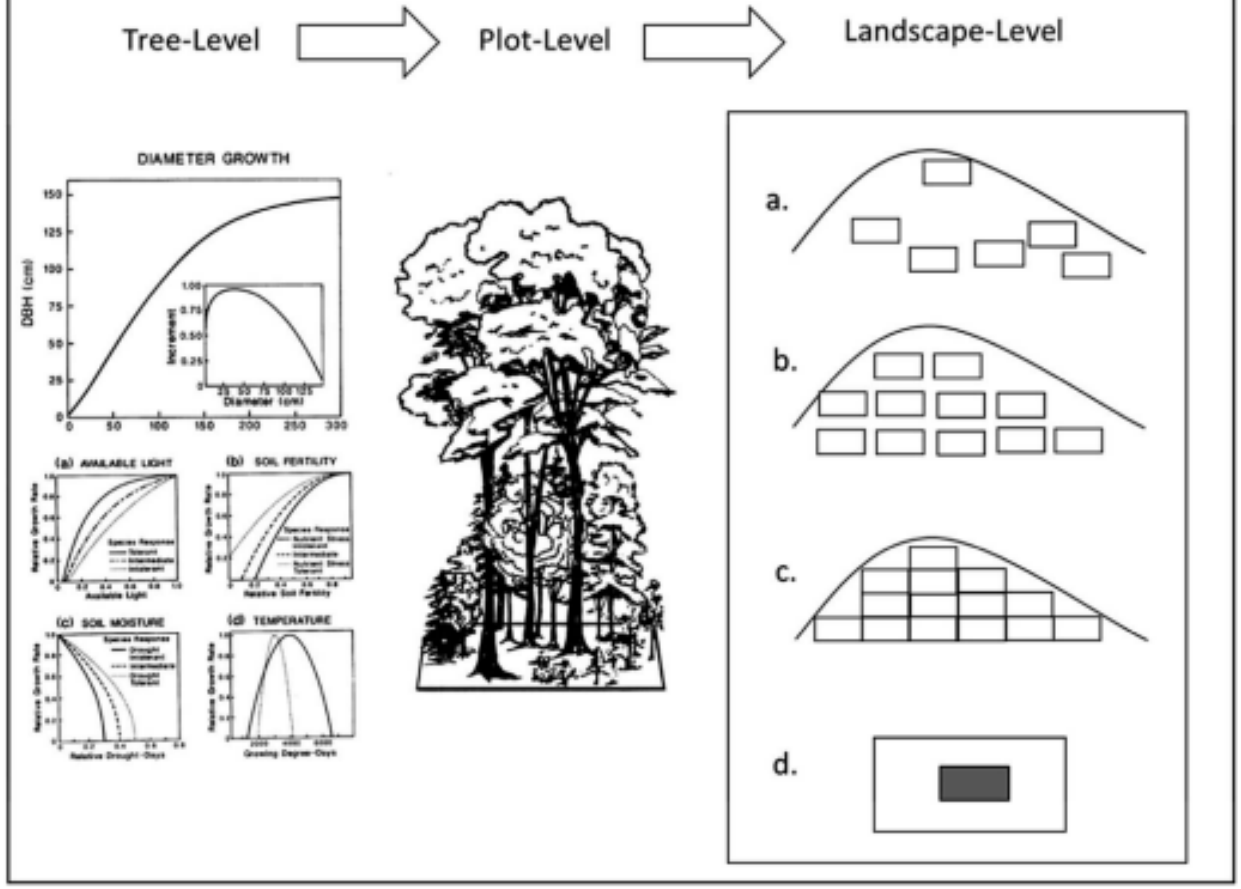

Figure 2. General functioning of a gap model. As one moves to the right to left, spatial scale increases from an individual tree to a small plot to a landscape. The tree-level response shown here is the elementary growth (or tree ring) equation from the FORET (Shugart and West 1977) model. The magnitude ot the tree-mortality probablity of each tree are also determined at the tree-level depending on tree growth as an index of vigor, species longevieties and other conditions. The form of the growth equation with no constraints is shown at the top and the decrement to this optimal growth equation is found below according to the particular controlling environmental factors (available light, soil moisture, etc). At the plot level, the vertical profile of light, available soil moisture, and other environmental and biogeochemical factors are calculated and tree to tree interactions are computed. Conditions for potential new seedlings for each year are determined factors such as the environmental conditions and seed sources. At the landscape model, a basic gap model can be used to represent the landscape as: (*a*) the summation of a Monte Carlo collection of independent random points; (*b*) gridded points at some spacing, (*c*) a tessellation of adjacent plots; (*d*) a spatially explicit landscape simulation with a spatial map of trees that is 'windowed' or updated for tree birth, growth and death by dropping a gap-model computational window onto the tree-stem map to solve for a subset of a new map. This is repeated to produce the new map. The size of this subset determines the resolution of the spatial map.

Shugart, H. H., Wang, B., Fischer, R., Ma, J., Fang, J., Yan, X., ... & Armstrong, A. H. (2018). Gap models and their individual-based relatives in the assessment of the consequences of global change. *Environmental Research Letters*, *13*(3), 033001.

Population Dynamics: Predator-Prey Relationship (

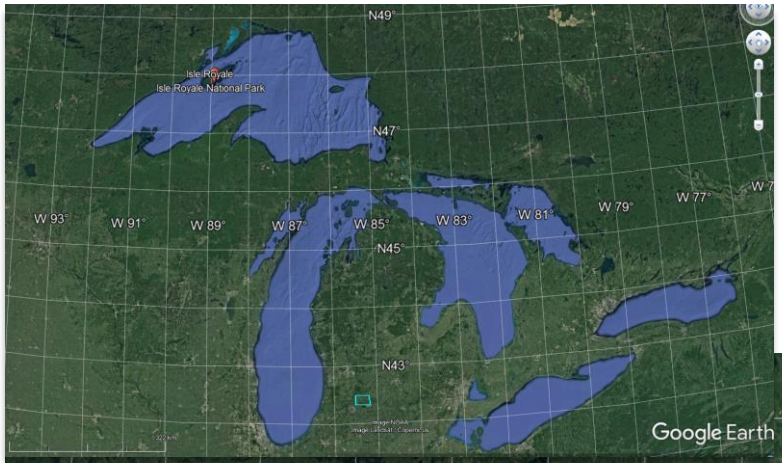

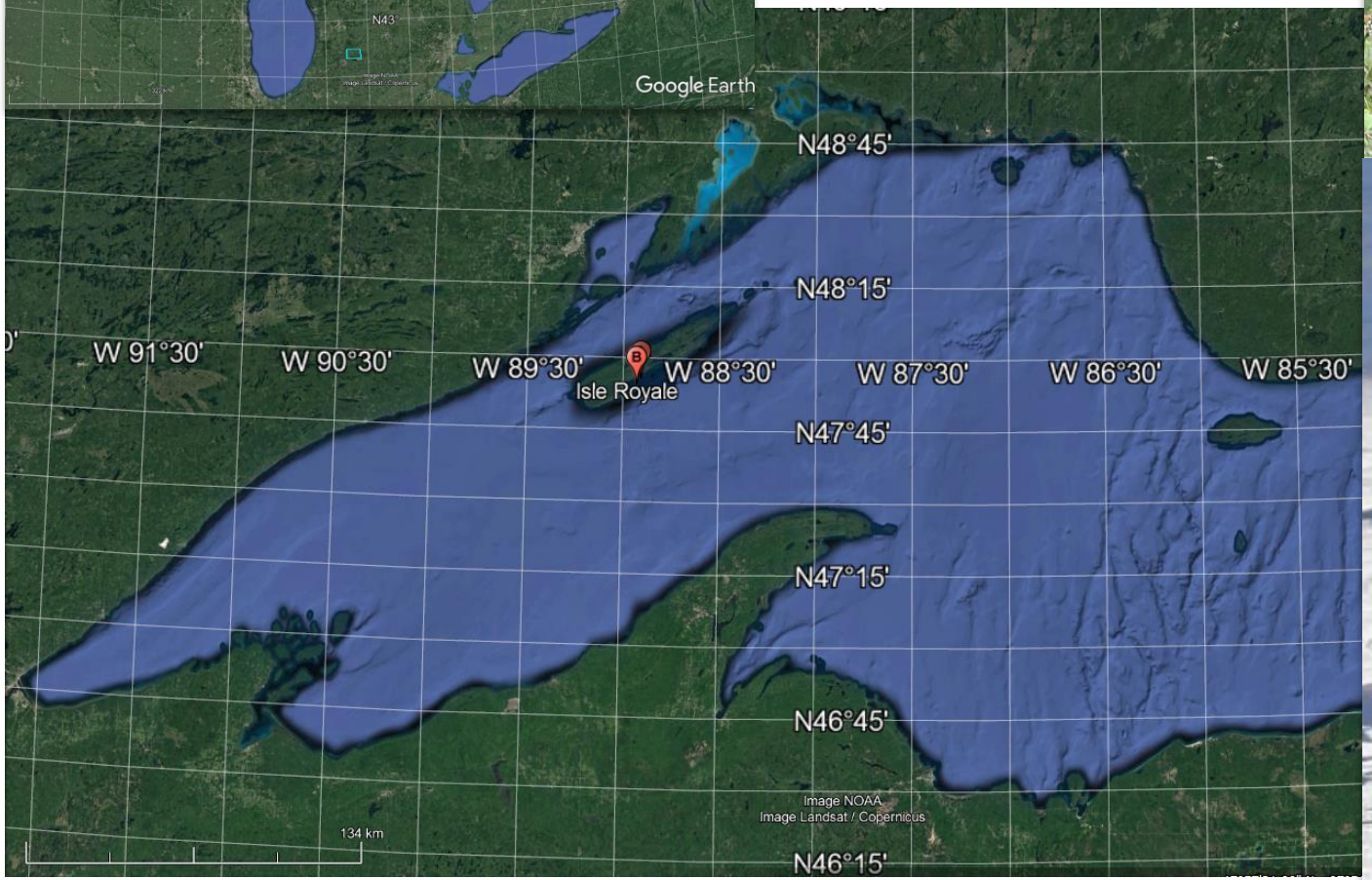

Population Dynamics: Predator-Prey Relationship (Wolf-Moose on Isle Royal National Park)

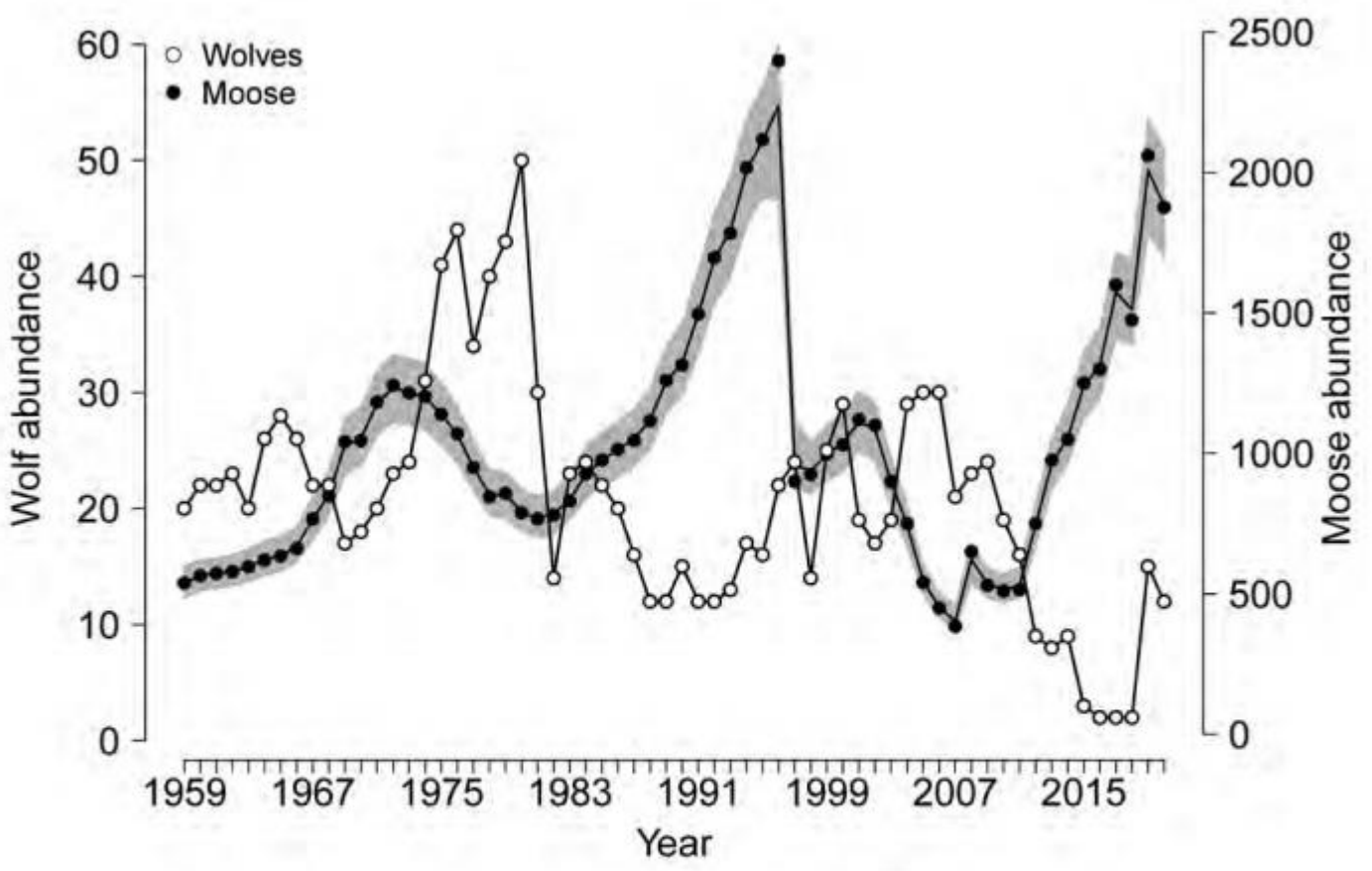

Figure 1. *Wolf and moose fluctuations in Isle Royale National Park, 1959–2020. Wolf abundances (open circles) were based on aerial surveys conducted from January to March. The sudden increase in wolf abundance in 2019 is the result of wolves being translocated by the National Park Service. Moose abundances (filled circles) during 1959–2001 are based on population reconstruction from the recoveries of dead moose, and estimates from 2002 to 2020 are based on aerial surveys. The second set of moose abundances (lines) and confidence intervals (shaded area) are results of a Bayesian state-space model that takes account of density dependence and age structure, as well as sampling error (Hoy et al. 2020,* Functional Ecology*). By contrast, confidence intervals reported in the main text emphasize sampling error associated with aerial surveys.*

The BIDE Model

Population = + Birth
+ ~~Immigration~~
+ Death
+ ~~Emigration~~

Death = function (Wolf Population)

https://www.youtube.com/watch?v=PdwnfPurXcs

Ecosystem Model

flows of mass and energy through an ecosystems

Fluxes among the components expressed as differential equations!

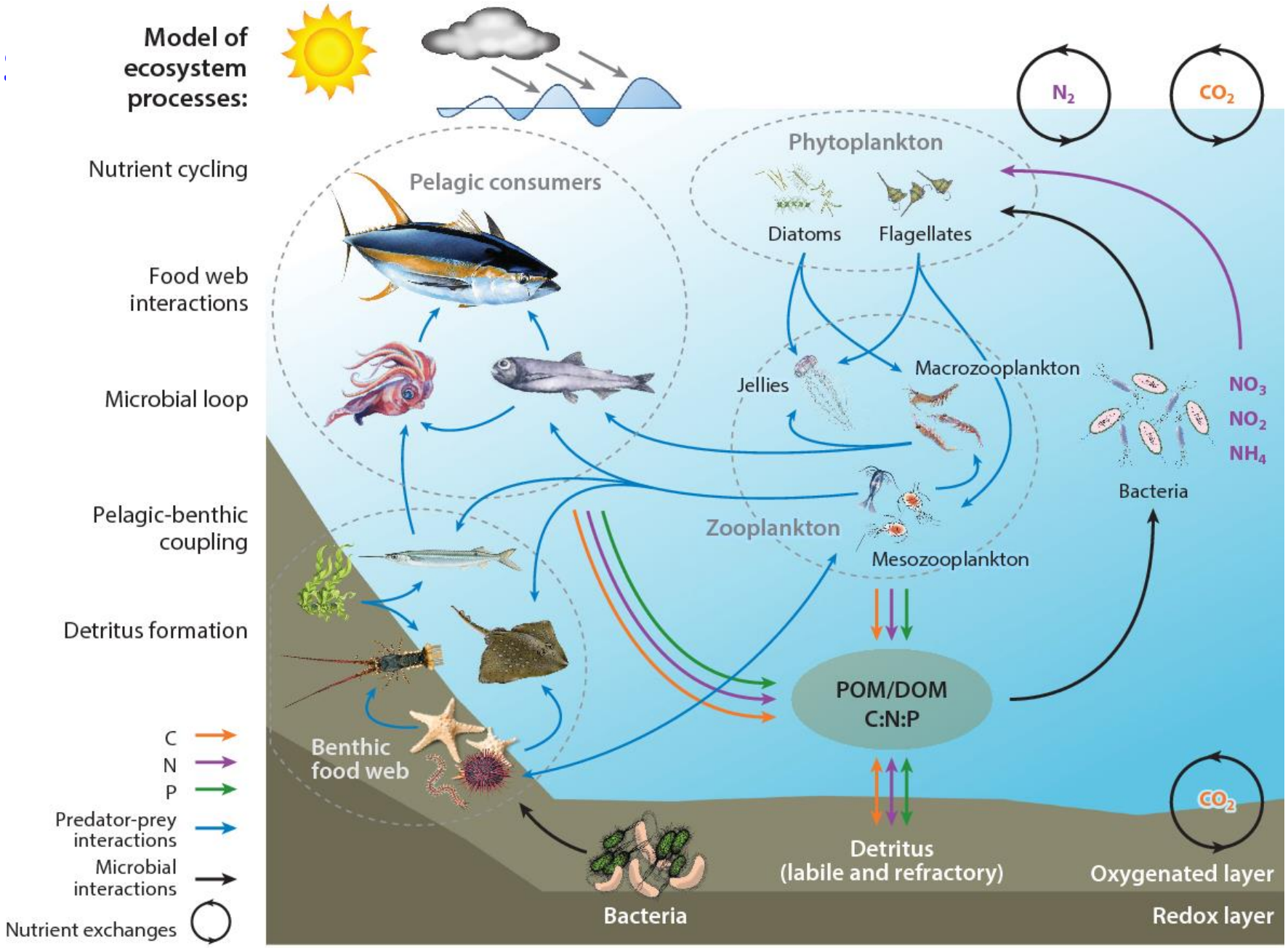

Pethybridge, H. R., Choy, C. A., Polovina, J. J., & Fulton, E. A. (2018). Improving marine ecosystem models with biochemical tracers. *Annual review of marine science*, *10*, 199-228.

Ecosystem Models: more examples

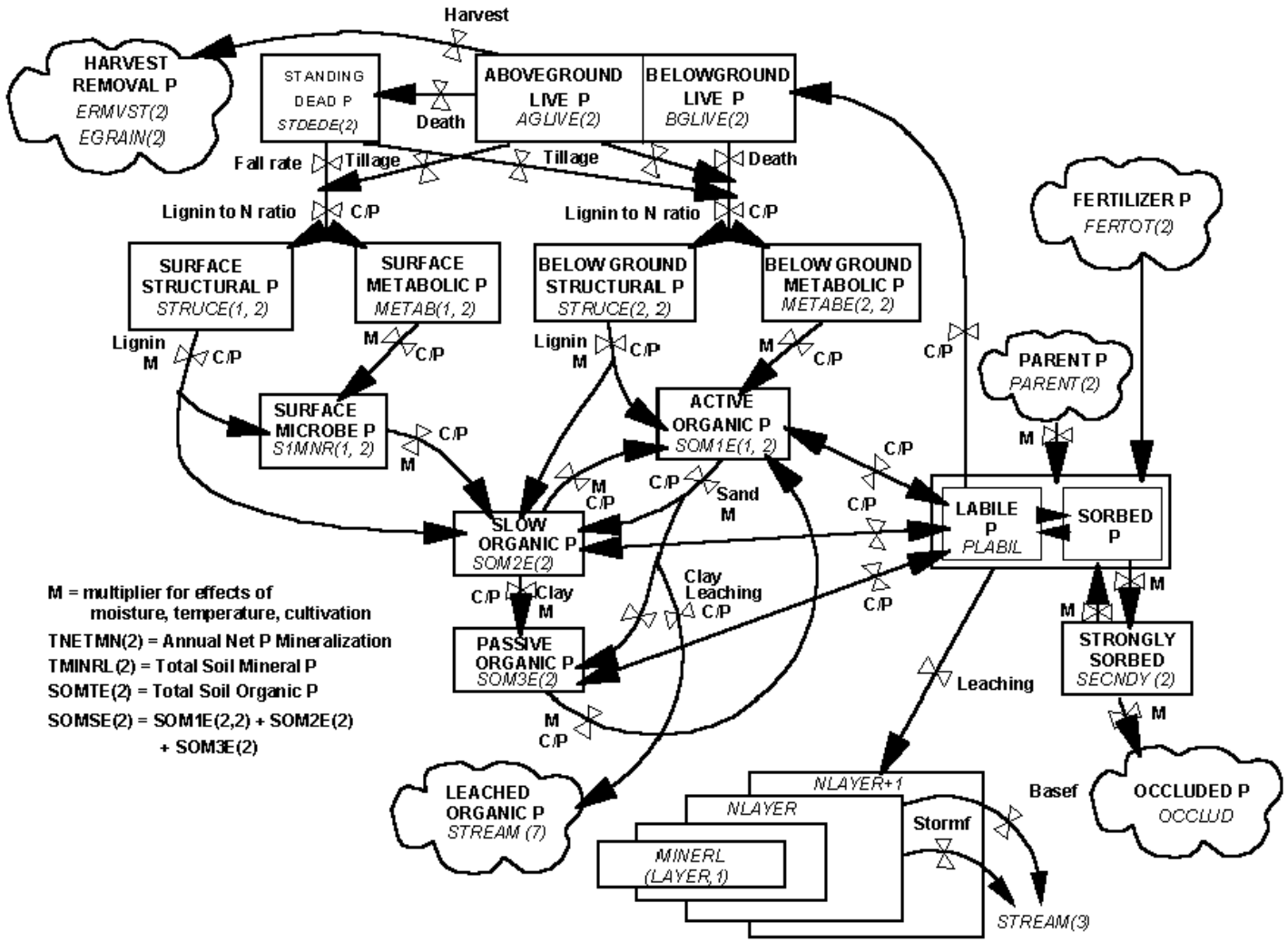

Open Source Codes

www2.nrel.colostate.edu/projects/century/MANUAL/html_manual/man96.html#INTRO

Apps jiquan chen - Googl... Jiquan Chen | Publo... Scopus preview - S... Ecological Processe... (14) Jiquan Chen | S... Coronavirus - Coro... MyAnalytics M

The command and previous value lines will continue to be shown until the user enters Q, to quit, or until the end of the option is reached.

[Previous Topic] [Next Topic] [Table of Contents]

4.5. Changing an Option

The user may change values of parameters within an existing option. After entering 2, for changing, the program will display each option which exists in the file and ask if the user would like to change that option:

Current option is W1 Wheat-type-one
Is this an option you wish to change

A response of "Y" or "y" will cause the program to move on to the change phase. If no option is responded to with a yes answer, the program will return to the previous menu of five actions. Once an affirmative response has been given, the user will be asked for a new abbreviation and description:

Enter a new abbreviation or a <return>
to use the existing abbreviation:

A new abbreviation must be unique to that file and no more than 5 characters; if a duplicate is entered, the user will be asked to enter another abbreviation.

Enter a new description or a <return>
to use the existing description:

The description may not be longer than 65 characters.

Then, for each value in that option, the program will display the existing value for that parameter and ask the user for a new value:

Commands: D F H L Q <new value> <return>
Name: PRDX(1) Previous value: 300
Enter response:

The user may enter any of these possible responses, as shown on the Command line:

see the definition of that parameter ..... enter D
find a specific parameter in that option ..... enter F
see a help message ..... enter H
list the next 12 parameters ..... enter L
quit, retaining the old values for
this and the remaining parameters
in this option ..... enter Q
take the old value ..... enter <return>
enter a new value ..... enter a new value

The command and previous value lines will continue to be shown until the user enters Q, to quit, or until the end of the file is reached. Finally, the user is asked if changes made should be saved:

Do you want to save the changes made?

If this is answered with "y" or "Y", the changed values will be saved. Otherwise, the changes will be lost.

[Previous Topic] [Next Topic] [Table of Contents]

4.6. Changing the <site>.100 File

PnET is a suite of three nested computer **models** which provide a modular approach to simulating the carbon, water and nitrogen dynamics of forest **ecosystems**. (https://daac.ornl.gov/cgi-bin/dsviewer.pl?ds_id=817)

Aber, J.D., S.V. Ollinger, C.T. Driscoll, C.A. Federer, and P.B. Reich. 2005. PnET Models: Carbon, Nitrogen, Water Dynamics in Forest Ecosystems (Vers. 4 and 5). ORNL DAAC, Oak Ridge, Tennessee, USA. https://doi.org/10.3334/ORNLDAAC/817

https://www.researchgate.net/publication/232688300_Nor_Gloom_of_Night_A_New_Conceptual_Model_for_the_Hubbard_Brook_Ecosystem_Study/figures?lo=1

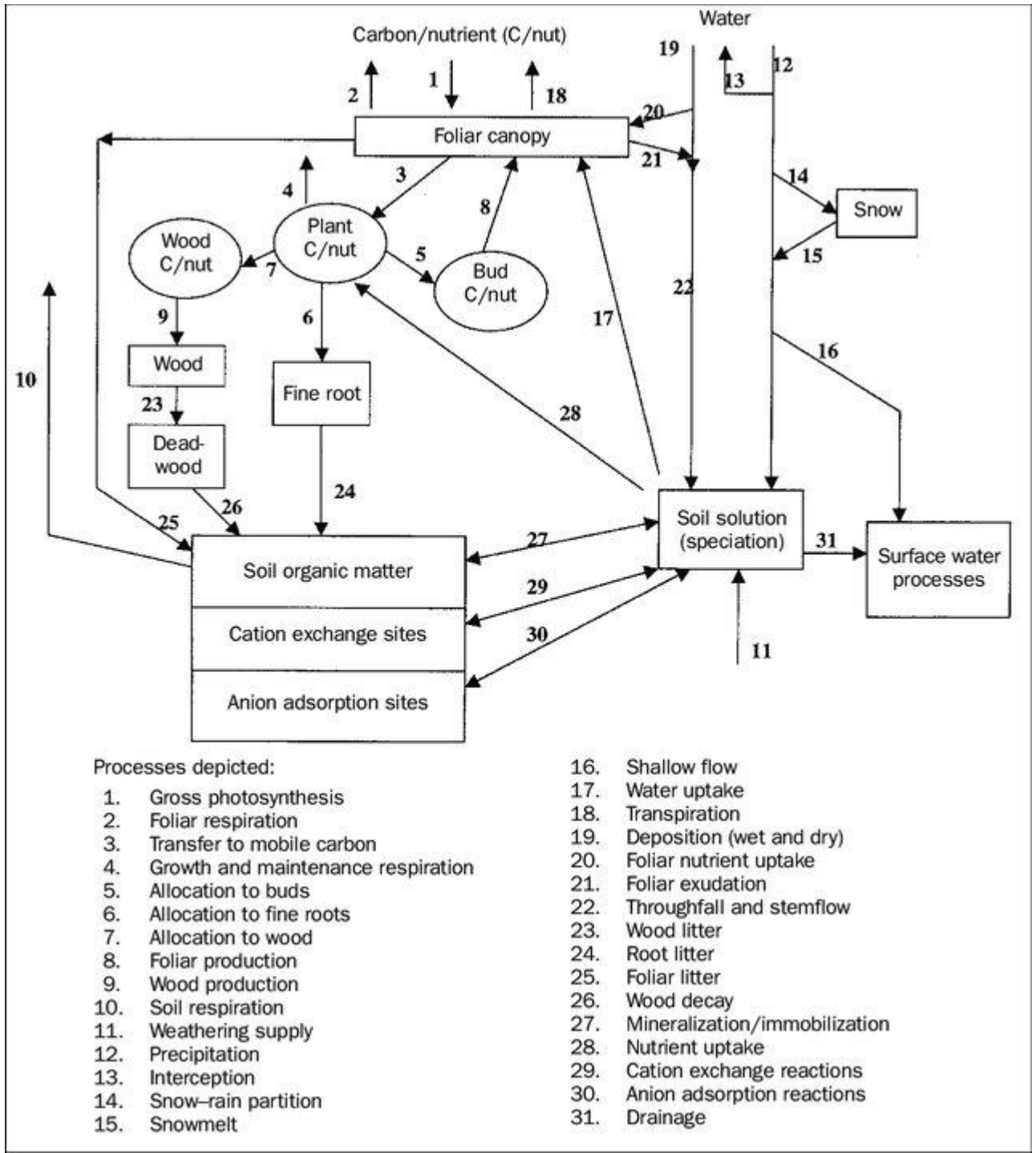

What is an Earth System Model (ESM)?

A coupled climate model is a computer code that estimates the solution to differential equations of fluid motion and thermodynamics to obtain time and space dependent values for temperature, winds and currents, moisture and/or salinity and pressure in the atmosphere and ocean. Components of a climate model simulate the atmosphere, the ocean, sea, ice, the land surface and the vegetation on land and the biogeochemistry of the ocean.
https://soccom.princeton.edu/content/what-earth-system-model-esm

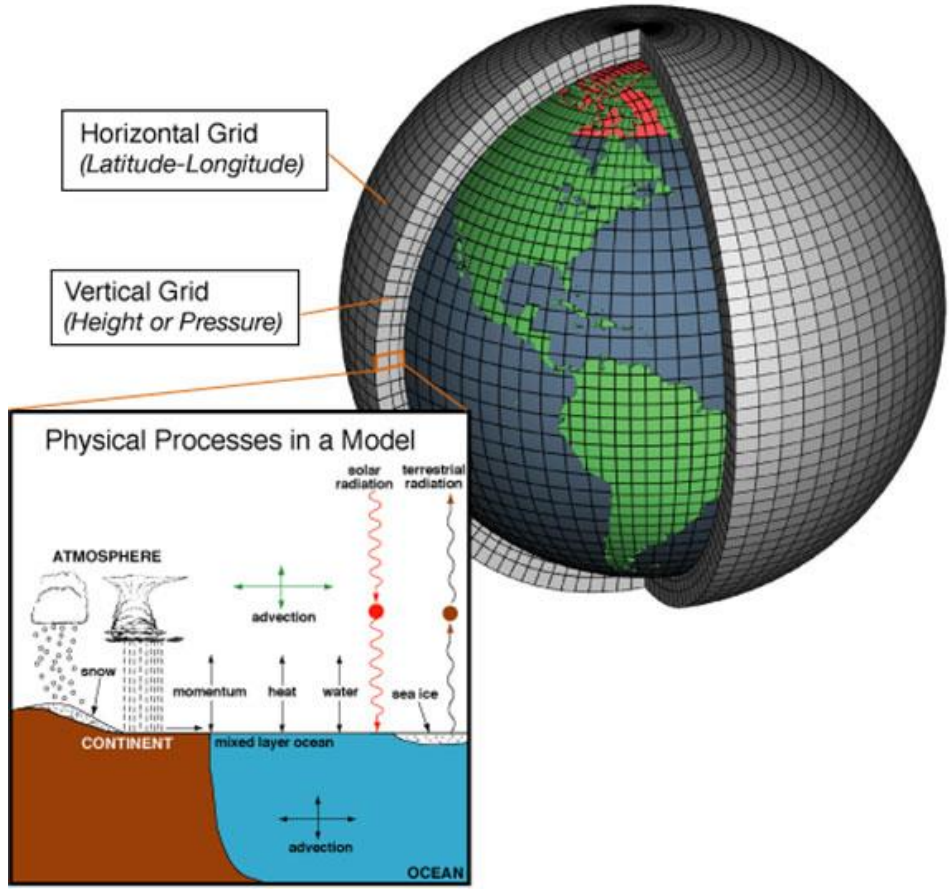

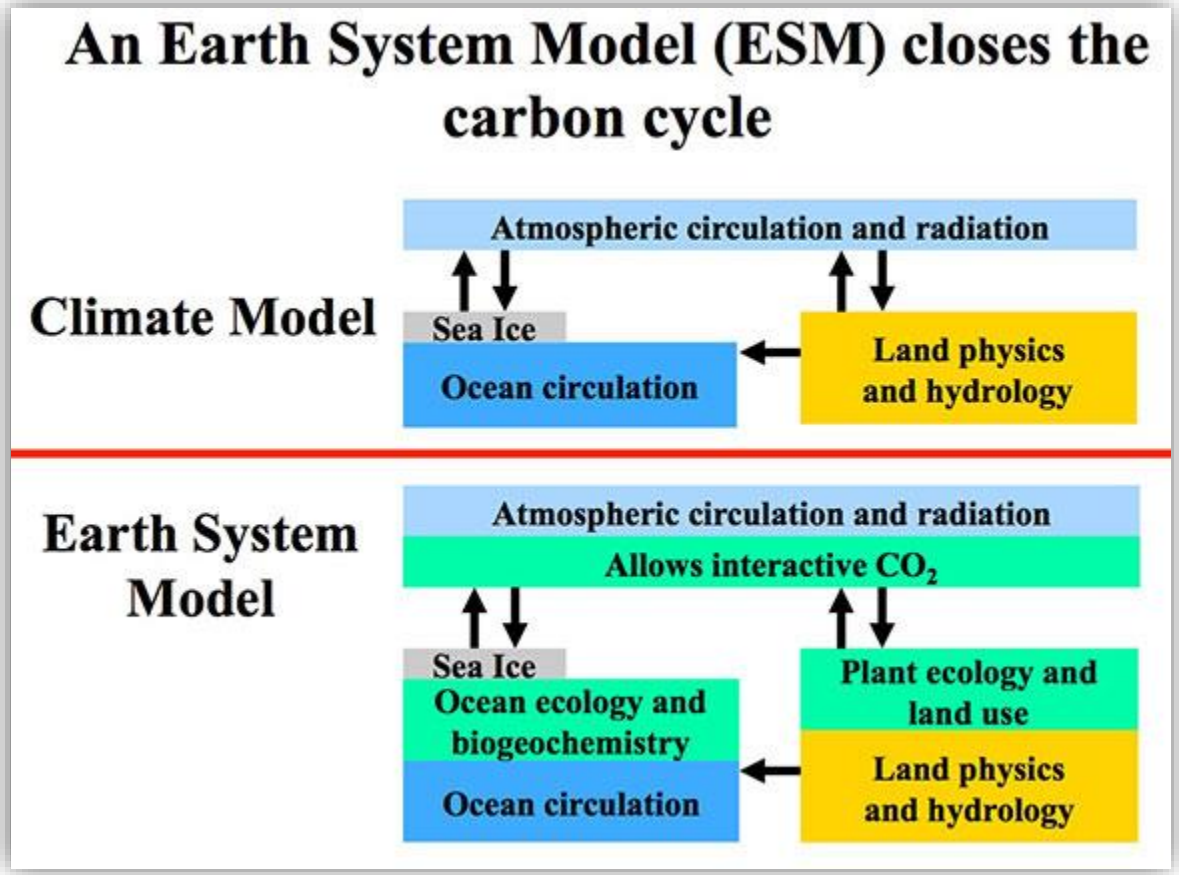

COMMUNITY LAND MODEL (CLM): the land model for the Community Earth System Model (CESM).

The model represents several aspects of the land surface including surface heterogeneity and consists of components or submodels related to land biogeophysics, the hydrologic cycle, biogeochemistry, human dimensions, and ecosystem dynamics. Specific processes that are represented include:

- Vegetation composition, structure, and phenology
- Absorption, reflection, and transmittance of solar radiation
- Absorption and emission of longwave radiation
- Momentum, sensible heat (ground and canopy), and latent heat (ground evaporation, canopy evaporation, transpiration) fluxes
- Heat transfer in soil and snow including phase change
- Canopy hydrology (interception, throughfall, and drip)
- Snow hydrology (snow accumulation and melt, compaction, water transfer between snow layers)
- Soil hydrology (surface runoff, infiltration, redistribution of water within the column, sub-surface drainage, groundwater)
- Plant hydrodynamics
- Stomatal physiology and photosynthesis
- Lake temperatures and fluxes
- Dust deposition and fluxes
- Routing of runoff from rivers to ocean
- Volatile organic compounds emissions
- Urban energy balance and climate
- Carbon-nitrogen cycling
- Dynamic landcover change
- Land management including crops and crop management and wood harvest
- Ecosystem Demography (FATES, optional)

Need a supercomputer to run!

http://www.cesm.ucar.edu/models/clm/

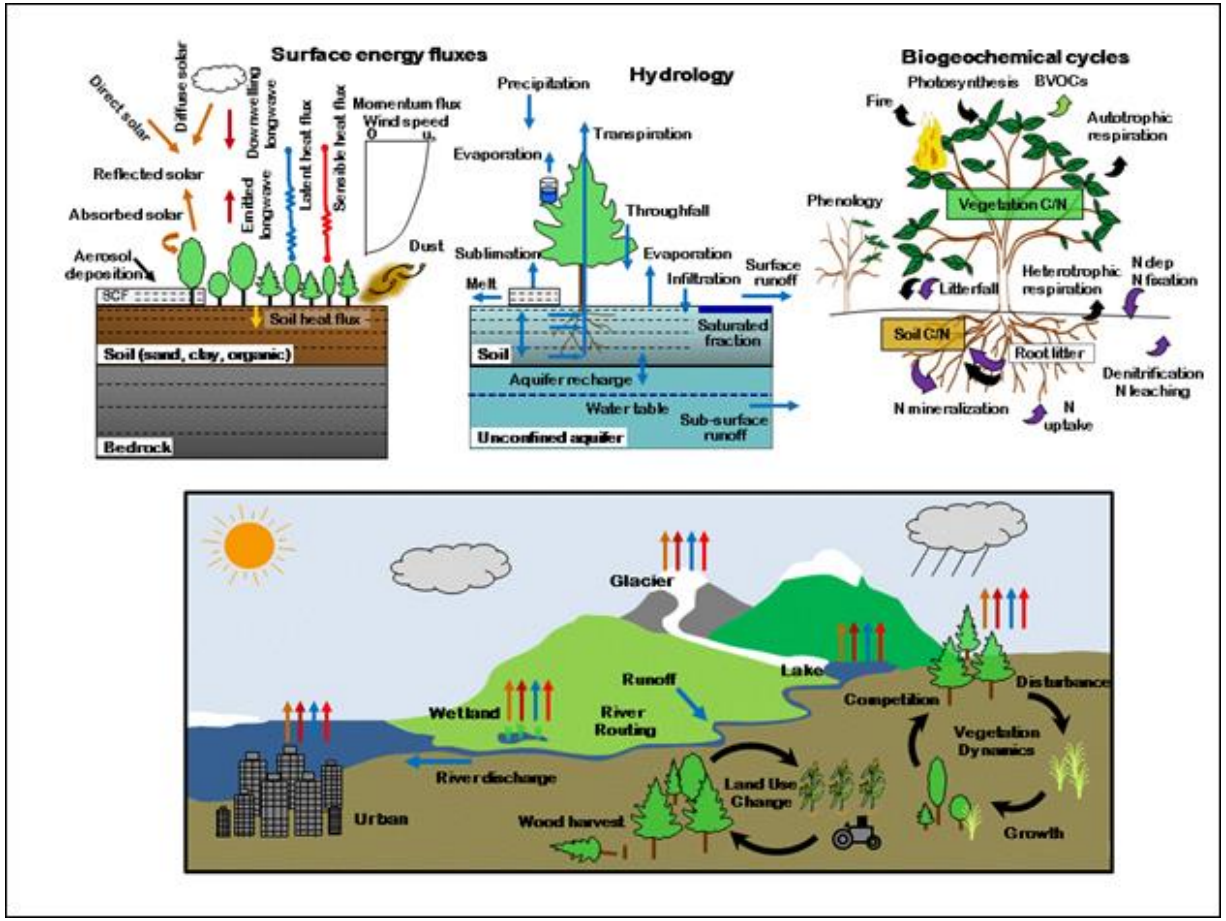

Schaefer, K., Schwalm, C. R., Williams, C., Arain, M. A., Barr, A., Chen, J. M., ... & Humphreys, E. (2012). A model-data comparison of gross primary productivity: Results from the North American Carbon Program site synthesis. *Journal of Geophysical Research: Biogeosciences*, *117*(G3).

Table 2. Summary of Model Characteristics

Model	Number Sites	Time Step	Soil Layers[a]	Phenology[b]	Nitrogen Cycle	GPP Model[c]	Leaf-to-Canopy	Reference
AgroIBIS	5	Hourly	11	Prognostic	Yes	EK	Big-Leaf	*Kucharik and Twine* [2007]
BEPS	10	Daily	3	Semi-prognostic	Yes	EK	2-Leaf	*Liu et al.* [1999]
Biome-BGC	33	Daily	1	Prognostic	Yes	EK	2-Leaf	*Thornton et al.* [2005]
Can-IBIS	24	Hourly	7	Prognostic	Yes	EK	2-Leaf	*Liu et al.* [2005]
CN-CLASS	28	Hourly	3	Prognostic	Yes	EK	2-Leaf	*Arain et al.* [2006]
DLEM	30	Daily	2	Semi-prognostic	Yes	EK	2-Leaf	*Tian et al.* [2010]
DNDC	5	Daily	10	Prognostic	Yes	LUE	Big-Leaf	*Li et al.* [2010]
Ecosys	35	Hourly	15	Prognostic	Yes	EK	2-Leaf	*Grant et al.* [2009]
ED2	24	Hourly	9	Prognostic	Yes	EK	2-Leaf	*Medvigy et al.* [2009]
EDCM	9	Daily	10	Prognostic	Yes	LUE	Big-Leaf	*Liu et al.* [2003]
ISAM	13	Hourly	10	Prognostic	Yes	LUE	2-Leaf	*Yang et al.* [2009]
ISOLSM	9	Hourly	20	Observed	No	EK	2-Leaf	*Riley et al.* [2002]
LoTEC	10	Hourly	14	Prognostic	No	EK	Big-Leaf	*Hanson et al.* [2004]
LPJ	26	Daily	2	Prognostic	No	EK	Big-Leaf	*Sitch et al.* [2003]
MODIS_5.0	38	Daily	0	Observed	No	LUE	Big-Leaf	*Heinsch et al.* [2003]
MODIS_5.1	37	Daily	0	Observed	No	LUE	Big-Leaf	*Heinsch et al.* [2003]
MODIS_alg	39	Daily	0	Observed	No	LUE	Big-Leaf	*Heinsch et al.* [2003]
ORCHIDEE	32	Hourly	2	Prognostic	No	EK	Big-Leaf	*Krinner et al.* [2005]
SiB3	28	Hourly	10	Observed	No	EK	Big-Leaf	*Baker et al.* [2008]
SiBCASA	32	Hourly	25	Semi-prognostic	No	EK	Big-Leaf	*Schaefer et al.* [2009]
SiBcrop	5	Hourly	10	Prognostic	Yes	EK	Big-Leaf	*Lokupitiya et al.* [2009]
SSiB2	39	Hourly	3	Observed	No	EK	Big-Leaf	*Zhan et al.* [2003]
TECO	32	Hourly	10	Prognostic	No	EK	2-Leaf	*Weng and Luo* [2008]
TRIPLEX	6	Daily	0	Observed	Yes	LUE	Big-Leaf	*Peng et al.* [2002]

[a]Zero soil layers indicate the model does not have a prognostic submodel for soil temperature and moisture.
[b]Observed phenology means the model uses remote sensing data to determine leaf area index (LAI) and gross primary productivity (GPP). Semi-prognostic means that remote sensing data is used to specify either LAI or GPP, but not both.
[c]GPP model types: EK (enzyme kinetic) and LUE (light use efficiency).

4. Conclusions

[42] None of the models in this study match estimated GPP within the range of uncertainty of observed fluxes. On average, the models achieved good performance for only 12% of the simulations. Two models achieved overall marginal performance, matching estimated GPP within roughly two times the uncertainty. Our first hypothesis proved false: we found no statistically significant differences in performance due to model structure, mainly due to the large spread in performance among models and across sites. The models in our study reproduced the observed seasonal pattern with little or no GPP in winter and peak GPP in summer, but did not capture the observed GPP magnitude. We found, on average, that models overestimated GPP in spring and fall and underestimated GPP in summer. Our second hypothesis proved true: model performance depended on how models represented the GPP response to changing environmental conditions. We identified three areas of model improvement: simulated LUE, low temperature response function, and GPP response under dry conditions.

[43] The poor overall model performance resulted primarily from inadequate representation of observed LUE. Simulated LUE is controlled by the leaf-to-canopy scaling strategy and a small set of model parameters that define the maximum potential GPP, such as ε_{max} (light use efficiency), V_{cmax} (unstressed Rubisco catalytic capacity) or J_{max} (the maximum electron transport rate). The temperature, humidity, and drought scaling factors determined temporal variability in simulated GPP, but the LUE parameters determined the magnitude of simulated GPP. To improve simulated GPP, model developers should focus first on improving the leaf-to-canopy scaling and the values of those model parameters that control the LUE.

[44] Many models overpredicted GPP under dry conditions, explaining why, on average, models performed worse at grassland and savanna sites than at forest sites. The importance of this to model performance increases at sites where drier conditions occur more frequently. Since dry conditions occur more frequently at grassland and savanna sites than at forest sites, models tended to perform worse at grassland and savanna sites compared to forest sites. Improving how models simulate soil moisture, drought stress, or humidity stress can improve simulated GPP under dry conditions.

[45] Many models overpredicted GPP under cold conditions, partly explaining the positive bias in simulated GPP in winter, spring, and fall. The estimated GPP completely shut down for daily average temperatures less than −6°C, but the Q_{10} formulation used by many models did not shut down GPP under cold or frozen conditions. The simulated GPP started too early in spring and persisted too late in fall, resulting in a positive bias and phasing errors in phenology. Using an ensemble mean can cancel out errors in phenology, but does not cancel out bias. Improving or imposing a low temperature inhibition function in the GPP model will resolve the problem.

Good News

Now there are a variety of system models that predict the magnitudes and dynamics of ecosystem properties. Each of these models was carefully constructed with sound algorithms from meteorological, hydrological, ecological, biogeochemical, and/or statistical principles. As a result, they are complex in terms of the number of processes factored, as well as regarding the inter-connections among the processes. Understanding and applying these models are not easy due to their complexity. Fortunately, almost all ecosystem models were developed with a few common algorithms. For example, Farquhar's photosynthesis equation, the Ball–Berry stomatal conductance algorithm, Michaelis–Menten kinetics, temperature-dependent respiration in the form of Q10, and energy balance are widely used. This book is designed to describe and explain the major biophysical and empirical modules that have been used in ecosystem models. Understanding these fundamental algorithms will speed up the application of system models. For model developers, knowledge about each of the crucial modules, including their varieties, behaviors and parameterization, model performances, and their strengths and limitations, is essential to improving and advancing their work. For example, a simple Q10 algorithm based on exponential equation (Chapter 3) has been widely used in many ecosystem models for calculating respiration, yet there are many other forms that may provide more realistic predictions, albeit requiring different sets of parameters. (Chen 2020, Preface)

Community Land Model (CML)

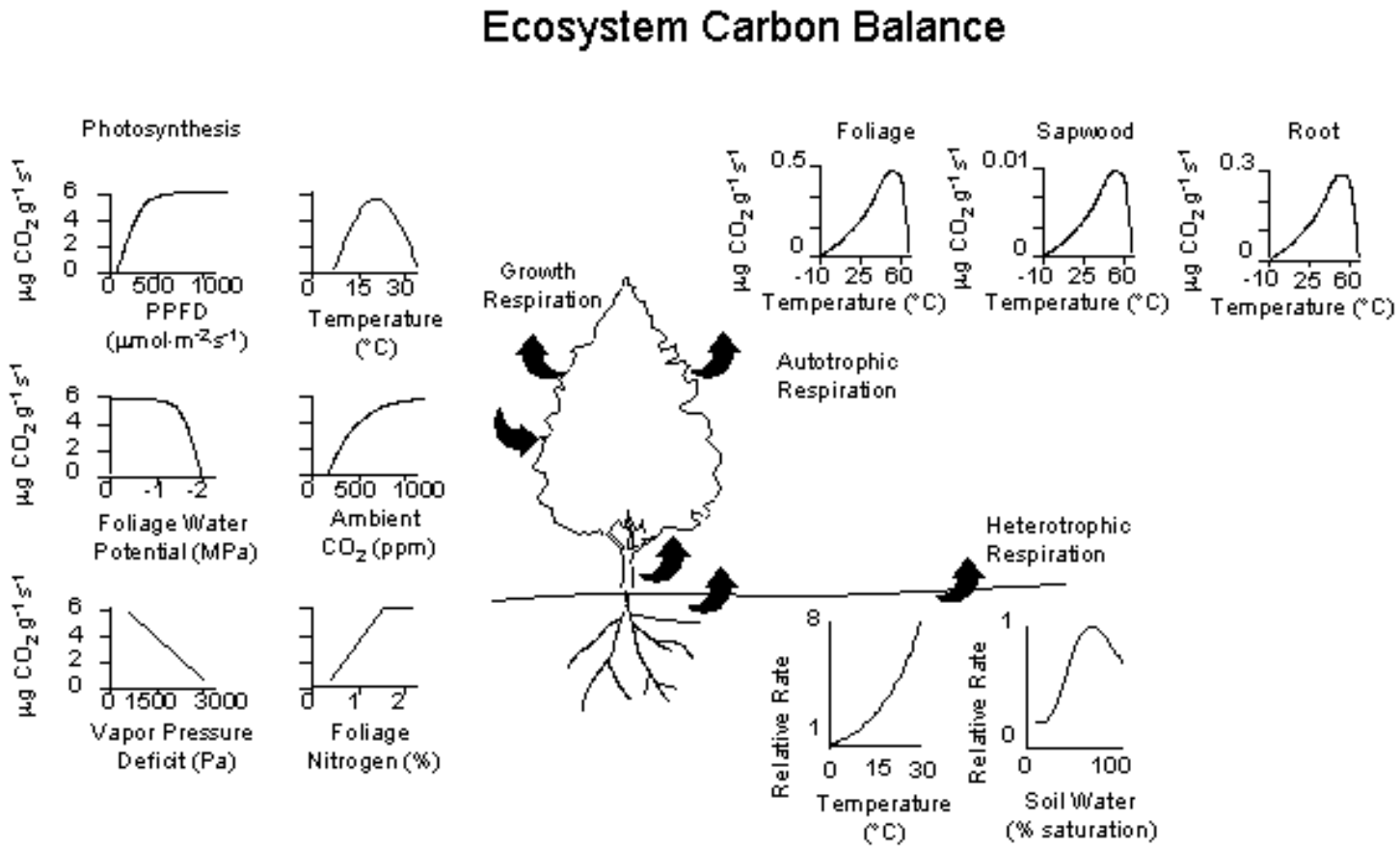

Computer Era models

- Increasing number of variables
- Mostly empirical relationships
- Climatic, soil, disturbances, management as regulations included
- Interactions among components (e.g., species, soil-plants) are considered
- Example: JOBAWA, FORET models (a.k.a. GAP models)

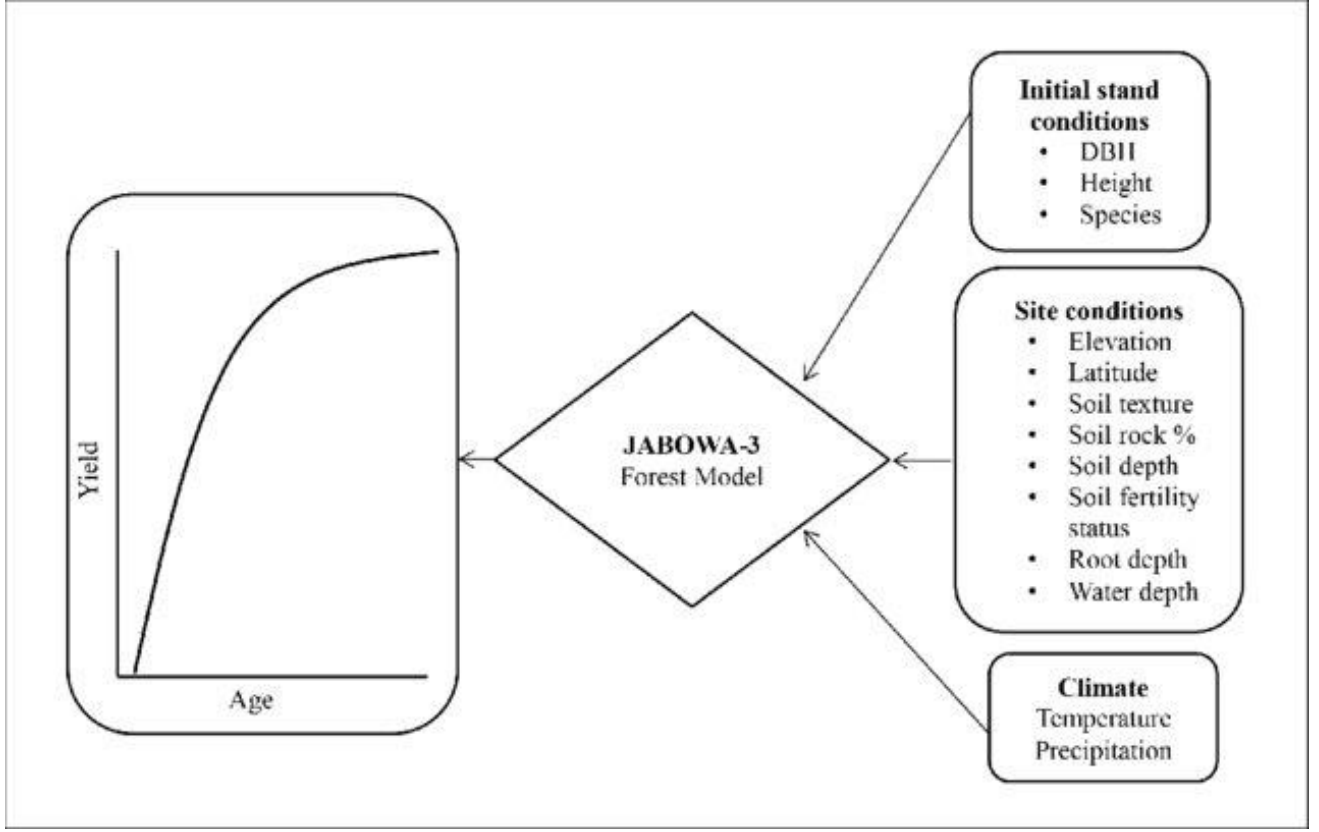

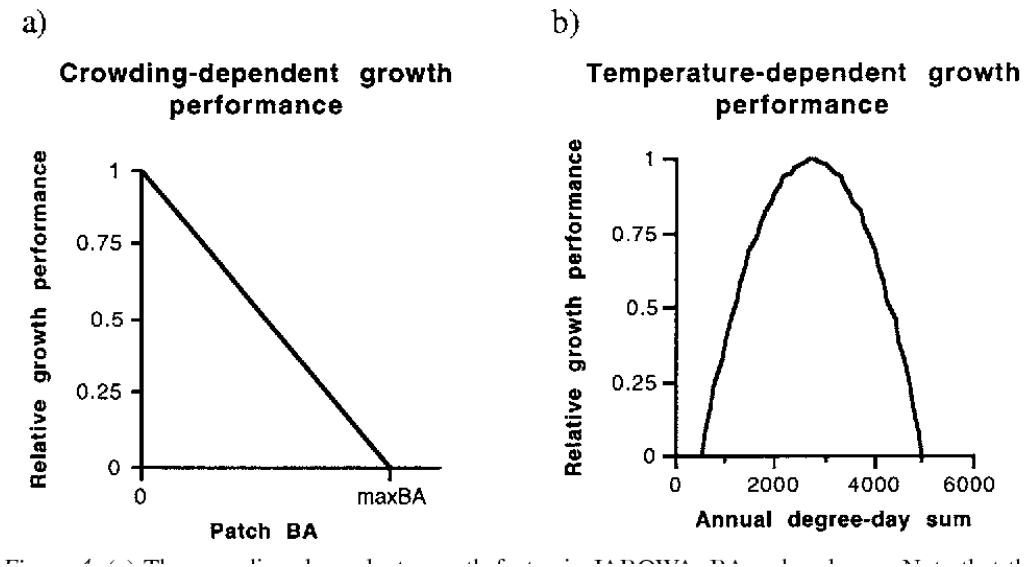

Ashraf, M. I., Bourque, C. P. A., MacLean, D. A., Erdle, T., & Meng, F. R. (2012). Using JABOWA-3 for forest growth and yield predictions under diverse forest conditions of Nova Scotia, Canada. *The Forestry Chronicle*, *88*(6), 708-721.

CLM5 Documentation
Feb 12, 2019

9.4 Photosynthesis

Photosynthesis in C_3 plants is based on the model of *Farquhar et al. (1980)*. Photosynthesis in C_4 plants is based on the model of *Collatz et al. (1992)*. *Bonan et al. (2011)* describe the implementation, modified here. In its simplest

form, leaf net photosynthesis after accounting for respiration (R_d) is

$$A_n = \min\left(A_c, A_j, A_p\right) - R_d. \tag{9.2}$$

The RuBP carboxylase (Rubisco) limited rate of carboxylation A_c (μ mol CO_2 m^{-2} s^{-1}) is

$$A_c = \left\{ \begin{array}{ll} \frac{V_{c\max}(c_i-\Gamma)}{c_i+K_c(1+o_i/K_o)} & \text{for } C_3 \text{ plants} \\ V_{c\max} & \text{for } C_4 \text{ plants} \end{array} \right\} \qquad c_i - \Gamma \geq 0. \tag{9.3}$$

The maximum rate of carboxylation allowed by the capacity to regenerate RuBP (i.e., the light-limited rate) A_j (μ mol CO_2 m^{-2} s^{-1}) is

$$A_j = \left\{ \begin{array}{ll} \frac{J_x(c_i-\Gamma)}{4c_i+8\Gamma} & \text{for } C_3 \text{ plants} \\ \alpha(4.6\phi) & \text{for } C_4 \text{ plants} \end{array} \right\} \qquad c_i - \Gamma \geq 0. \tag{9.4}$$

The product-limited rate of carboxylation for C_3 plants and the PEP carboxylase-limited rate of carboxylation for C_4 plants A_p (μ mol CO_2 m^{-2} s^{-1}) is

$$A_p = \left\{ \begin{array}{ll} 3T_p & \text{for } C_3 \text{ plants} \\ k_p \frac{c_i}{P_{atm}} & \text{for } C_4 \text{ plants} \end{array} \right\}. \tag{9.5}$$

For example

1) Michaelis-Menten kinetics for photosynthesis (GPP)

$$P_n = \frac{\alpha \cdot PAR \cdot P_m}{\alpha \cdot PAR + P_m} - R_d \qquad [2.2]$$

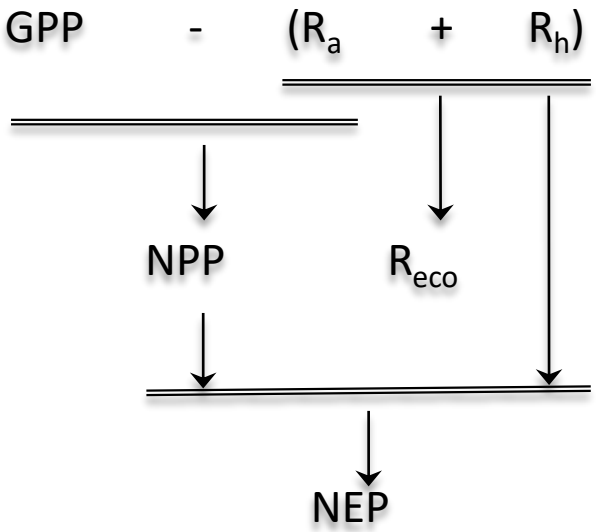

But with different varieties

$$P_n = \frac{1}{2 \cdot \beta}\left(\alpha \cdot PAR + P_m - \sqrt{(\alpha \cdot PAR + P_m)^2 - 4 \cdot \alpha \cdot PAR \cdot P_m \cdot \beta}\right) \qquad [2.4]$$

2) Q10 model for carbon loss (R_a, R_h, R_{eco}) in many models

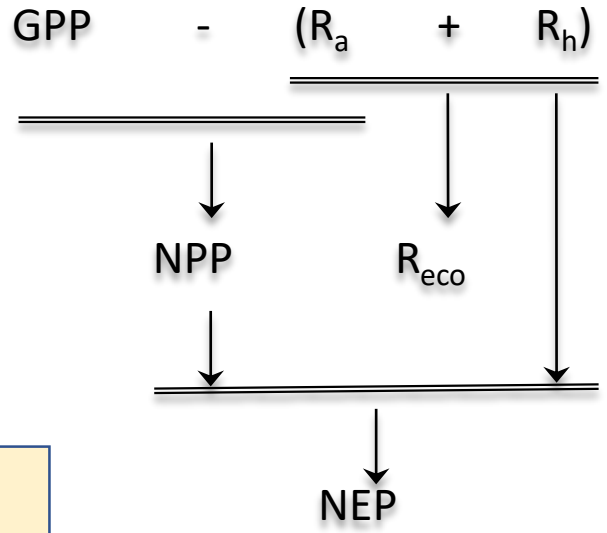

The Q_{10} model (Van't Hoff 1898):

$$Q_{10} = \left(\frac{R_2}{R_1}\right)^{\left(\frac{10}{T_2 - T_1}\right)}$$

Brief history
Principles
Strengths/weakness
Model demonstrations
…

But also with different varieties

$$R = R_0 \cdot e^{\beta_0 \cdot T} \cdot e^{\beta_1 \cdot \theta} \cdot \beta_2 \cdot T \cdot \theta \qquad [3.17]$$

PnET-II model

Vol. 5: 207–222, 1995 | CLIMATE RESEARCH Clim Res | Published December 7

Predicting the effects of climate change on water yield and forest production in the northeastern United States

John D. Aber[1,*], Scott V. Ollinger[1], C. Anthony Federer[2], Peter B. Reich[3], Michael L. Goulden[4], David W. Kicklighter[5], Jerry M. Melillo[5], Richard G. Lathrop, Jr[6]

Soil respiration: This routine was not present in the original model and is included here to allow a system-level carbon balance calculation. It does *not* contain a complete soil carbon budget which would be driven by litter deposition and associated decomposition terms. Rather, it uses a generalized soil respiration equation developed for temperate zone forests by Kicklighter et al. (1994). Soil respiration is assumed to include both microbial respiration associated with decomposition and respiration by live roots. That equation, derived using measured, plot-level soil CO_2 flux data from a wide variety of sites, is :

$$\text{Soil respiration (g C m}^{-2}\text{ mo}^{-1}) = 27.46\,e^{0.06844t} \quad (4)$$

where t is the mean monthly temperature (°C). Data from the Harvard Forest site represent approximately 24 % of the total used to derive this equation. The remaining data come from a widely distributed set of temperate zone forests (see Kicklighter et al. 1994 for full description).

It is also critical to lean how respiration is measured!

Figure 3-1. Schematic illustration of change in respiration with temperature by an exponential function (Eq. 3.3) for four Q_{10} values (a). The exponential increase of respiration can be limited by other ecological resources such as moisture (b). The respiration reduction due to low moisture can be linear, polynomial, Gamma, logistic, or take other forms. The threshold point can be empirically determined for a site or a specific time period.

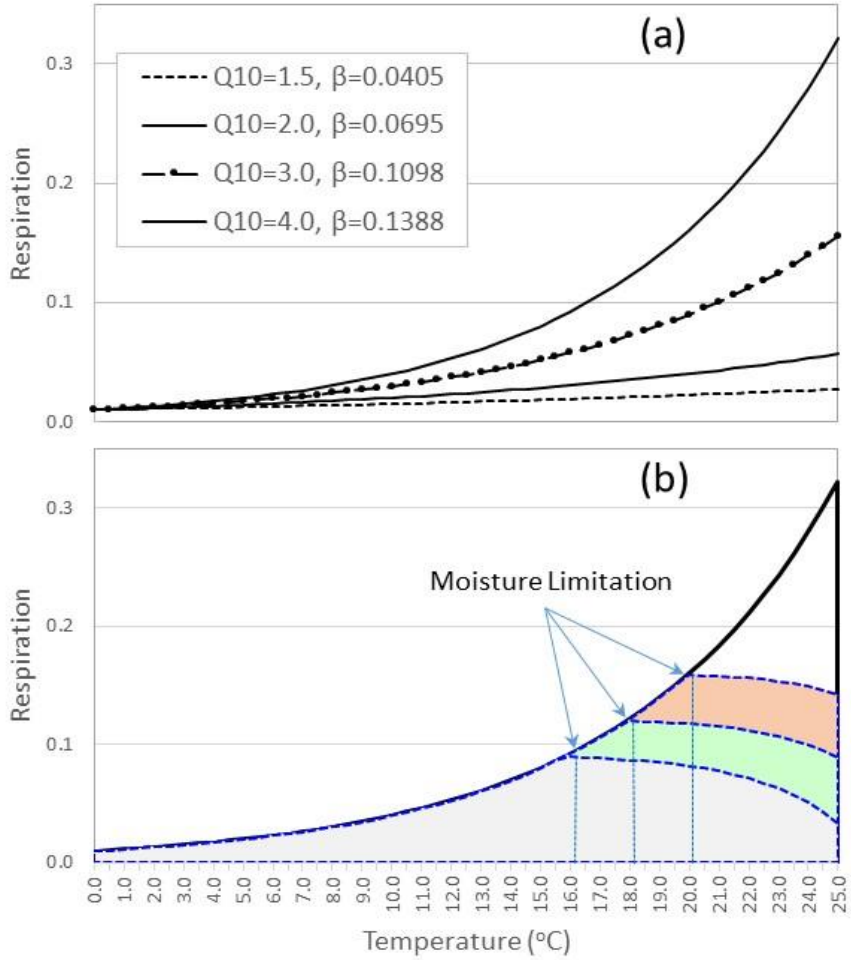

Hands on exercise is an effective way to learn!

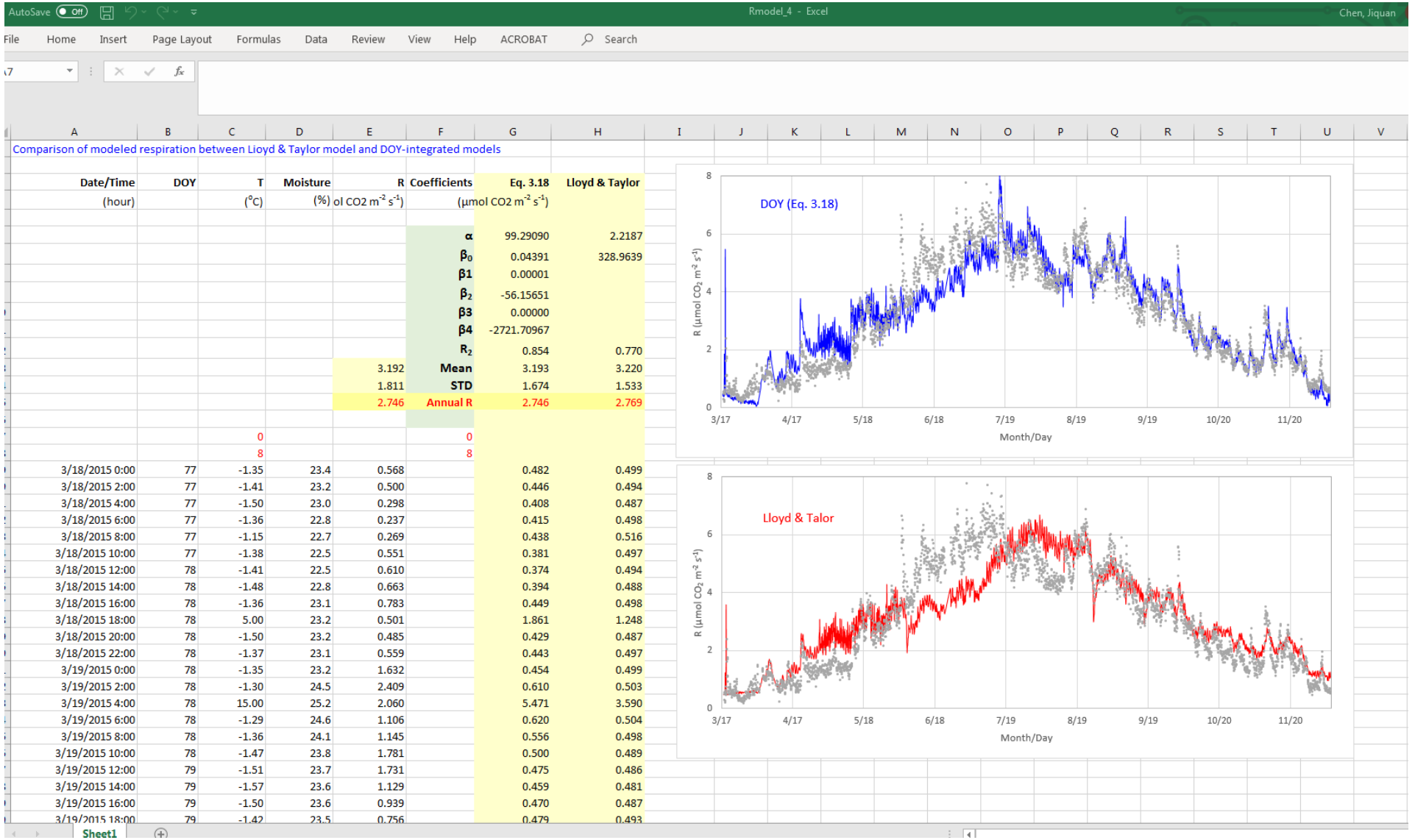

Biophysical Essentials For Ecosystem Models (Chapter 1)

1.2 Diurnal Changes of Air Temperature and Humidity

1.3 Atmosphere Water Vapor Pressure and VPD

1.4 Solar Radiation

1.5 Heat Storages in Soil, Air and Vegetation

1.6 Vertical Profile of Wind Speed

1.7 Energy Balance

- In-class demonstration of the solar model
- Additional resources
- Homework 1
- Handout 1: unit and conversions
- Handout 2: R codes for VPD calculations and graphing

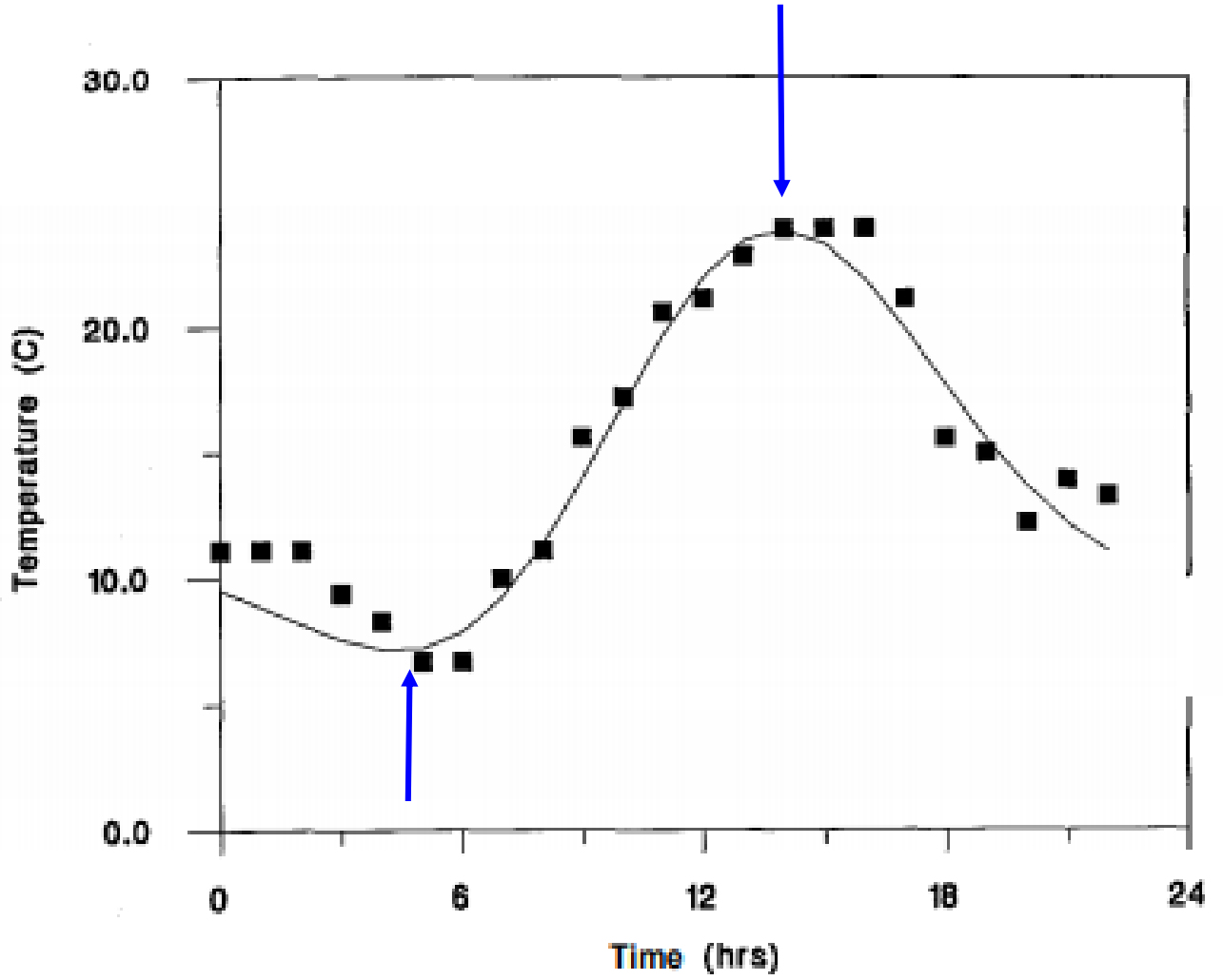

FIGURE 2.2. Hourly air temperature (points) on a clear fall day at Hanford, WA. The curve is used to interpolate daily maximum and minimum temperatures to obtain hourly estimates.

Notes:

- Air temperature is measured at 2 m above the ground (vegetation) by WMO standards
- When data are downloaded, please make sure Ta is measured at the same height
- 30 min or hourly means are often reported in microclimatic study, but historical data can be at 3-hour or even longer term
- Data use without specified scale and height can cause large errors for model predictions

Diel t° change

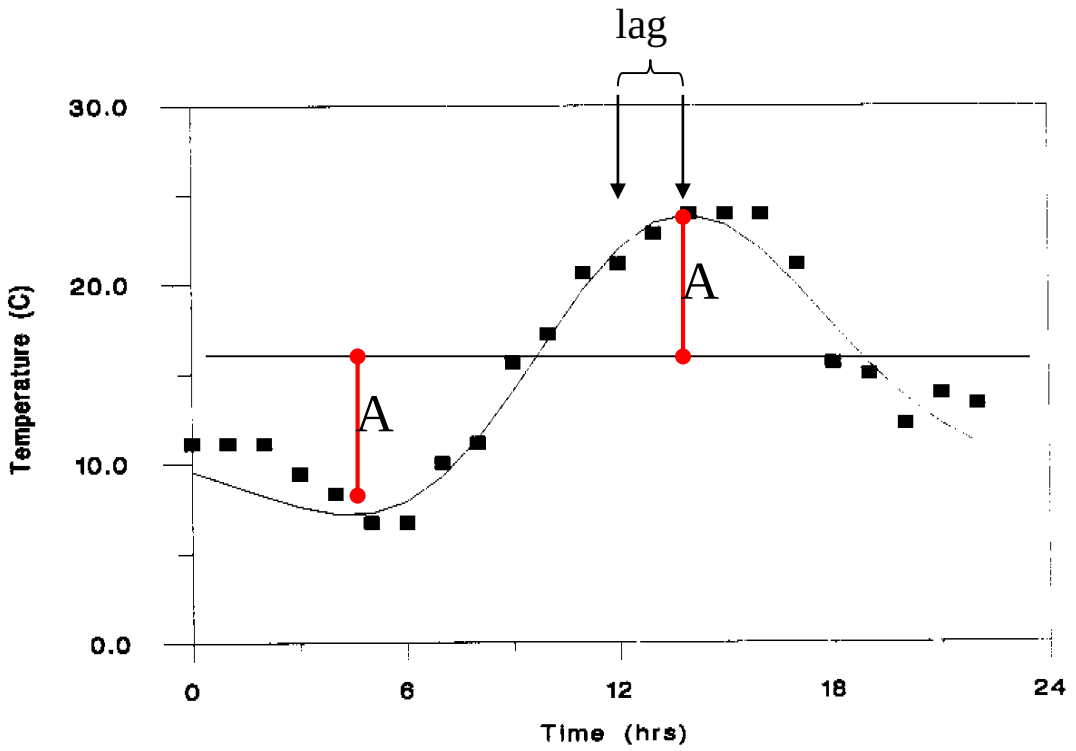

FIGURE 2.2. Hourly air temperature (points) on a clear fall day at Hanford, WA. The curve is used to interpolate daily maximum and minimum temperatures to obtain hourly estimates.

- t_{max} lags behind Φ_{max}
- Lag = f {d}
- Amplitude = f {d}

See S1-2 for modeling diel air temperature.

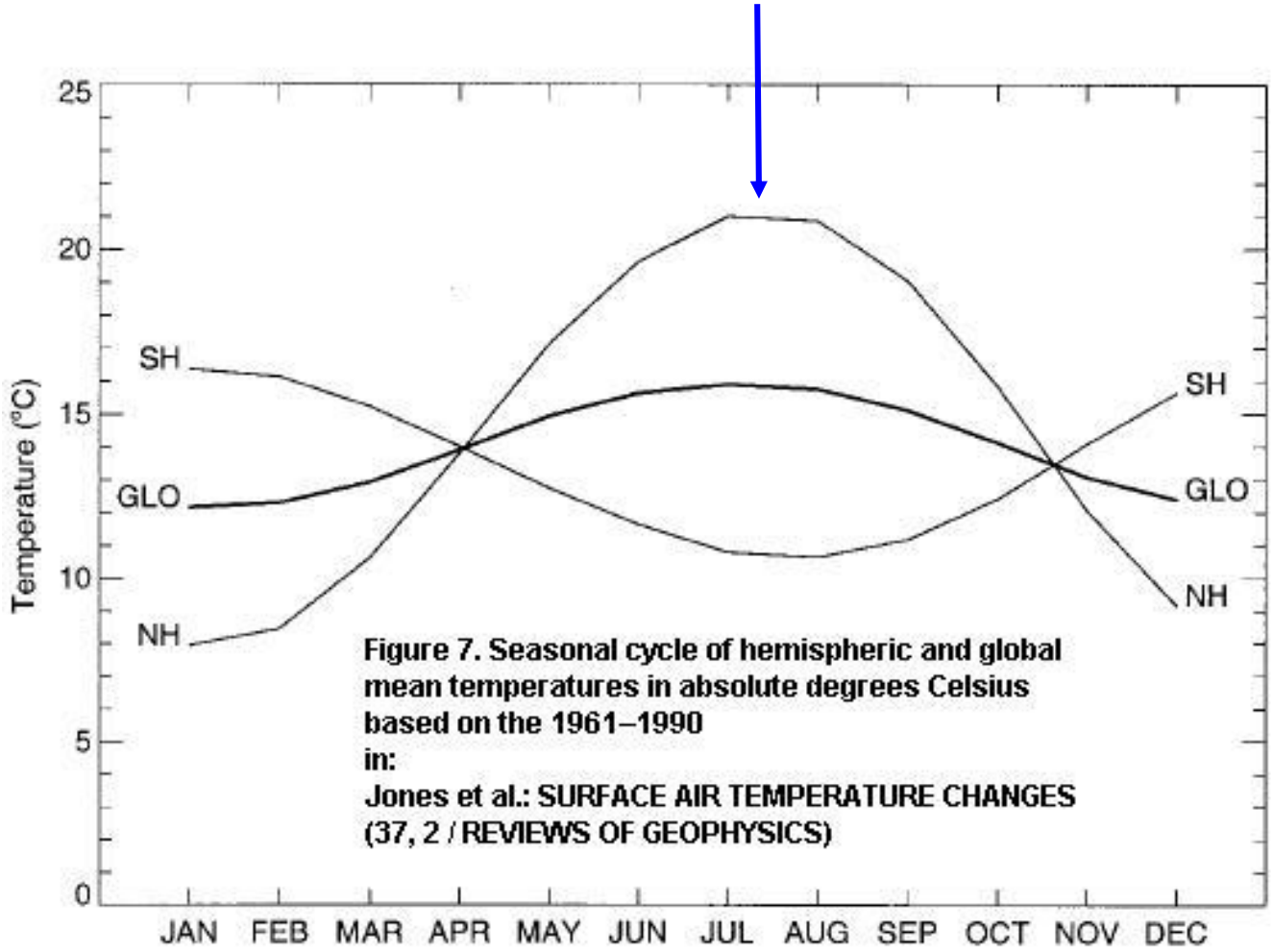

P. D. Jones et. al.: SURFACE AIR TEMPERATURE AND ITS CHANGES OVER THE PAST 150 YEARS (Seite 24 von 28 der PDF-Datei), CC BY-SA 3.0, https://commons.wikimedia.org/w/index.php?curid=9695907

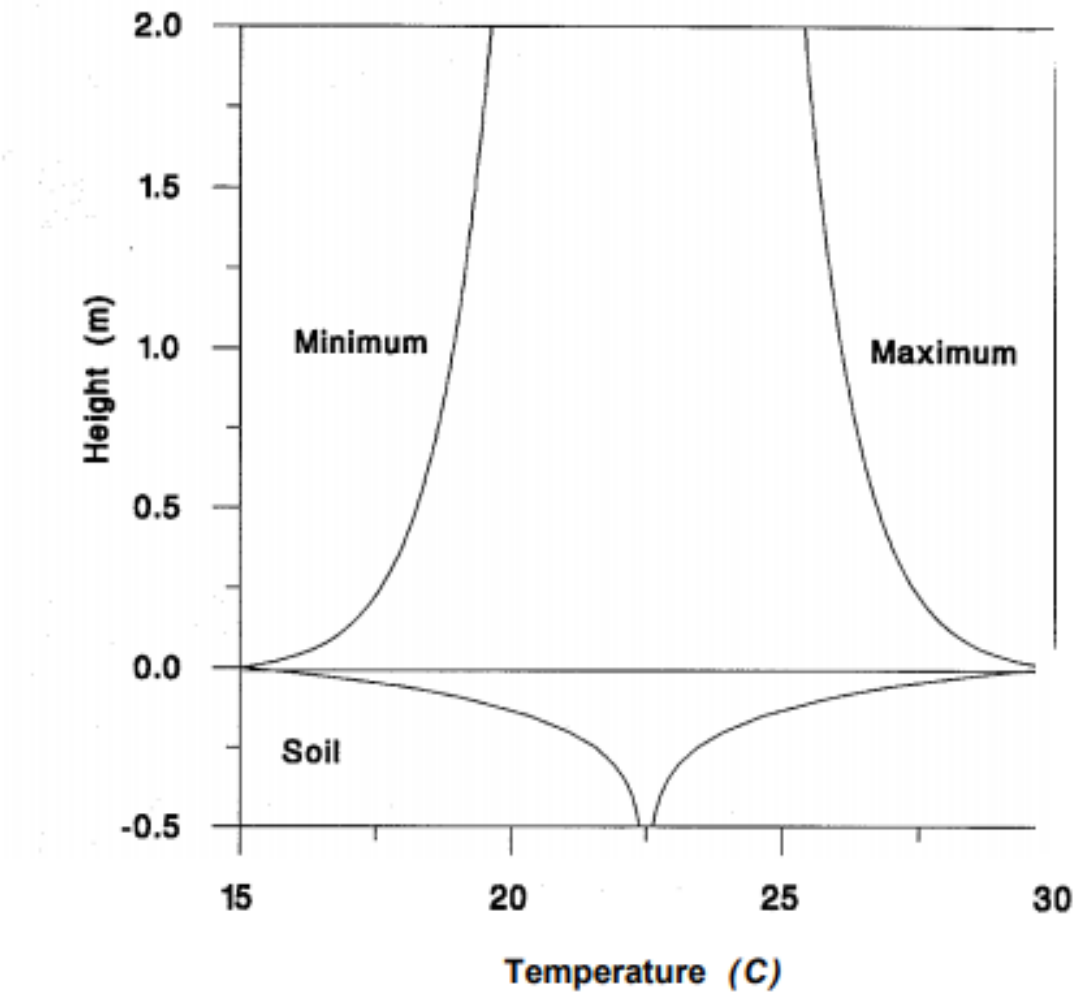

FIGURE 2.1. Hypothetical profiles of maximum and minimum temperature above and below soil surface on a clear, calm day.

Applications in Ecology, Agriculture, Forestry, etc.

- Growing degree days (the temperatures above which certain plant/animal growth occurs).
- Phenology (temperature > 3 ^{o}C for 3^{+} days)
- Growing season length (the average number of days a year with a 24-hour average temperature of > 5-6 °C)
- Biophysical models (e.g., Q10 model) (Lloyd & Taylor 1994) Chapter 3

$$R = k_R M = A e^{BT}$$ eqn 4

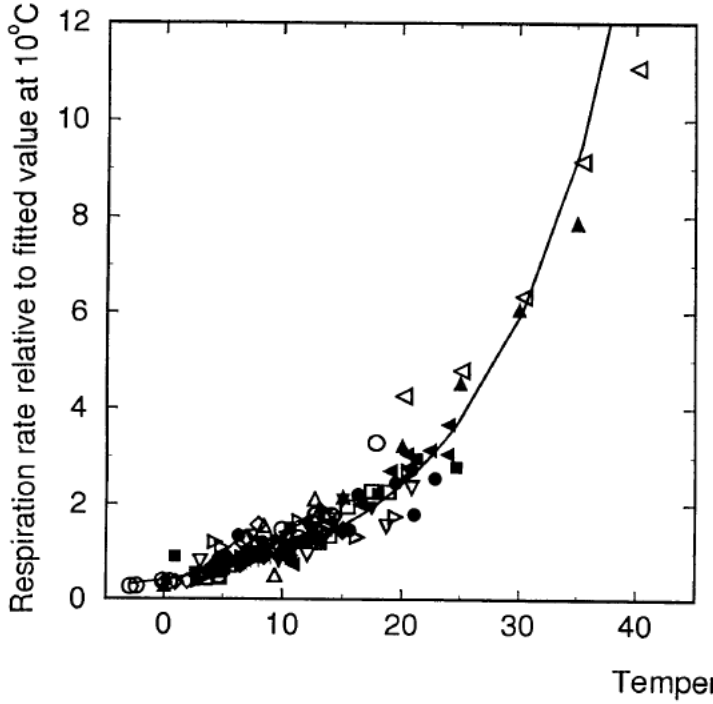

Fig. 2. Respiration rates (relative to the fitted value at 10 °C) a respiration rate and temperature (equation 6). Also shown is a Symbols are given in Table 1.

Diurnal changes in microclimate under different harvest regimes, (a) Patterns of shortwave radiation (kW/m^2) for a 70-year-old Douglas-fir (*Pseudotsuga menziesii*) forest (thick black line) and three sites recently harvested using clearcut (solid line with circles), dispersed green-tree retention (partial cut; solid line), and aggregated green-tree retention (patch; dashed line) techniques, (b) Patterns of air temperature (°C) at 2 m above the ground for the same sites. Data were collected in western Washington on 25 August 1992 (the study sites are shown in Figure 2).

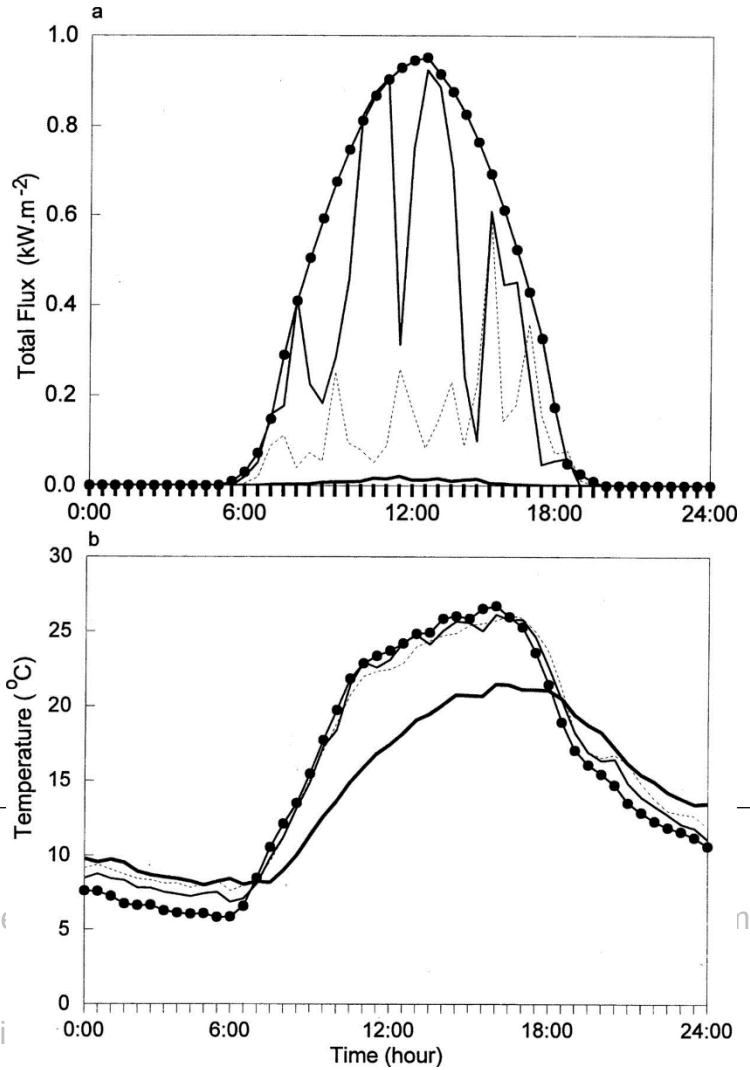

Diurnal changes in microclimatic variables at three landforms: ridge tops (solid black line), south- and west-facing slopes (thick gray line), and north- and east-facing slopes (thin black line). Variables monitored included (a) air temperature at 2 m height, (b) relative humidity, (c) shortwave radiation, (d) wind velocity, (e) air temperature at ground surface, and (f) soil temperature at 5 cm depth. Data were collected on 24 August 1995.

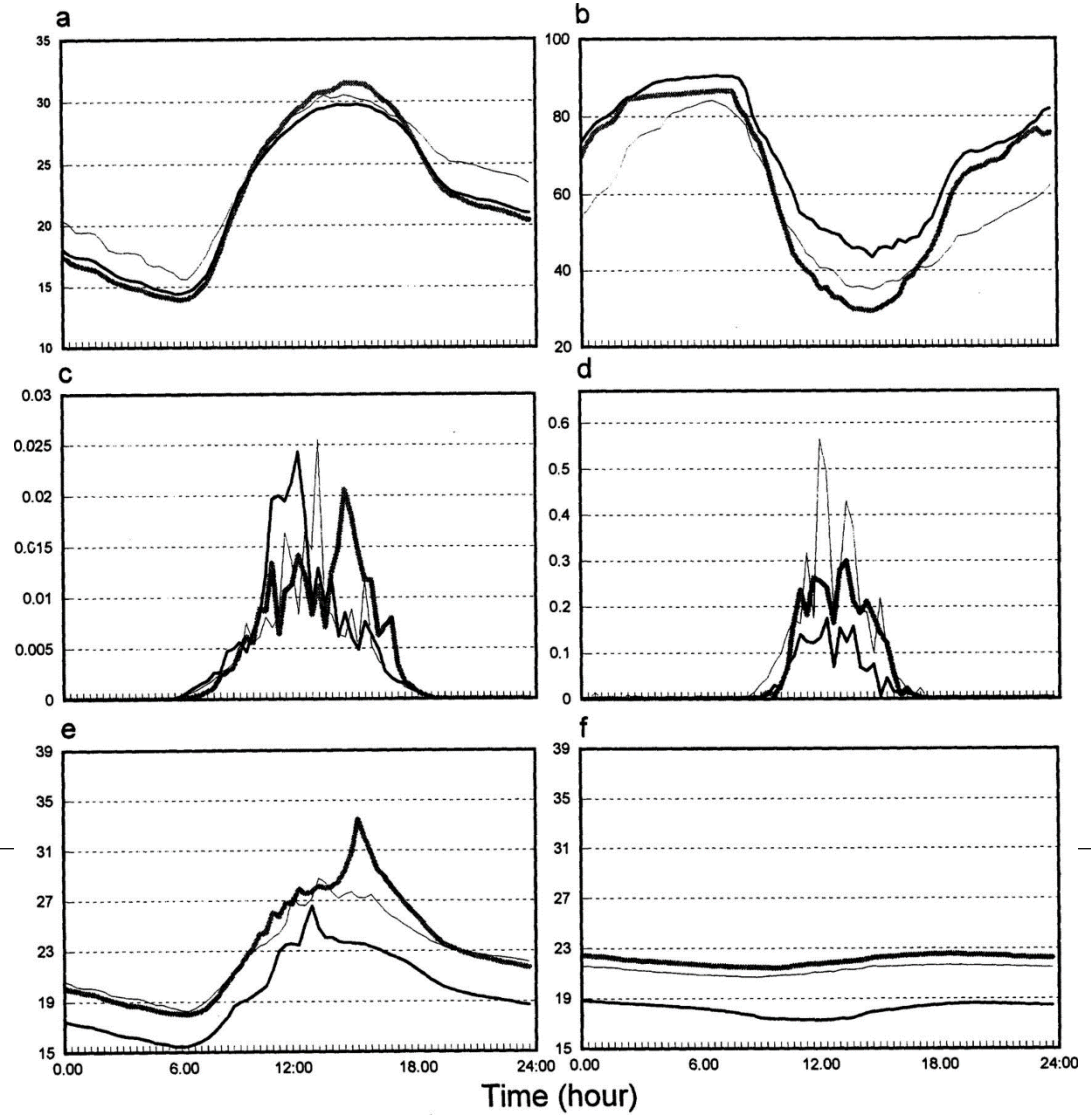

Water Vapor

Latent heat of vaporization

TABLE A2. Properties of water

T C	ρ_w MG/m^3	λ kJ/mol	ν mm^2/s	D_H mm^2/s	D_o mm^2/s	D_v mm^2/s
0	0.99987	45.0	1.79	0.134		
4	1.00000	44.8	1.57	0.136		
10	0.99973	44.6	1.31	0.140		
20	0.99823	44.1	1.01	0.144	0.002	0.002
30	0.99568	43.7	0.80	0.148		
40	0.99225	43.4	0.66	0.151		
50	0.98807	42.8	0.56	0.154		

Specific heat of water	75.4 J mol^{-1} C^{-1}
Latent heat of freezing	6.0 kJ mol^{-1}
Thermodynamic psycrometerconstant at 20 C	0.000664 C^{-1}

$\gamma = C_p/\lambda$

Vapor saturation

Saturation = f {T; P=f{A}}

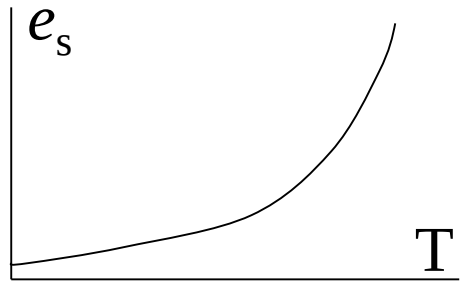

Tetens formula:

Coefficients chosen according to env. Conditions

For environ. biophys.:

- a=0.611 kPa
- b=17.502
- c=240.97°C

$$e_s(t) = a * \exp\left(\frac{bT}{T+c}\right)$$

Saturation pressure e_s roughly doubles for each 10°C increase:

$e_s(0°)$=0.611 kPa; $e_s(10°)$=1.23 kPa; $e_s(20°)$=2.34 kPa; $e_s(30°)$=4.24 kPa

Water Vapor (Fritzchen 1979, Chapter 6)

The *saturation deficit* or the *vapor pressure deficit*, VPD, is the difference between the saturation and actual vapor pressure at the same temperature and pressure. For example, at an air temperature of 29°C and vapor pressure of 2.005 kPa, the saturation vapor pressure is 4.005 kPa. Therefore the saturation deficit is 2.0 kPa.

The *relative humidity* of air, U, is the ratio in percent of water vapor of moist air relative to the saturation vapor pressure at the same temperature and pressure,

$$U = 100\left(\frac{e}{e_w}\right). \tag{6.13}$$

Relative humidity of 50%, labeled on the right axis of Fig. 6.1, represents the condition where the atmospheric vapor pressure is equal to one half of the saturation vapor pressure at that temperature. Both saturation vapor pressure and relative humidity may be defined with respect to a plane surface of ice. The saturation vapor pressure of ice at 0°C is practically equal to that over water at 0°C.

Water Vapor (Fritzchen 1979, Chapter 6)

The *dew point*, T_d, is the temperature at which saturation will occur if moist air is cooled at constant pressure. This is also the condition in which the relative humidity is 100% and condensation occurs. To find the dew-point temperature of air at 50% relative humidity and 29°C temperature locate the intersection of 50% and 29°C in Fig. 6.1 and follow the 2.0 kPa line horizontally to the left until the 100% relative humidity line is reached. The isotherm intersecting this point, 17.6°C, is the dew-point temperature.

The *wet-bulb* temperature, T_w, of moist air at a given pressure and air temperature is the temperature attained when the moist air is brought adiabatically to saturation by evaporation of water into the moist air. The wet-bulb temperature for air of 50% U and 29°C air (Fig. 6.1) is found by moving from the 50% and 29°C intersection upward to the left parallel to the diagonal lines until the 100% U line is reached. The isotherm intersecting this point, 21.2°C, is the wet-bulb temperature.

$$e_a = e_s(T_w) - \gamma p_a(T_a - T_w)$$

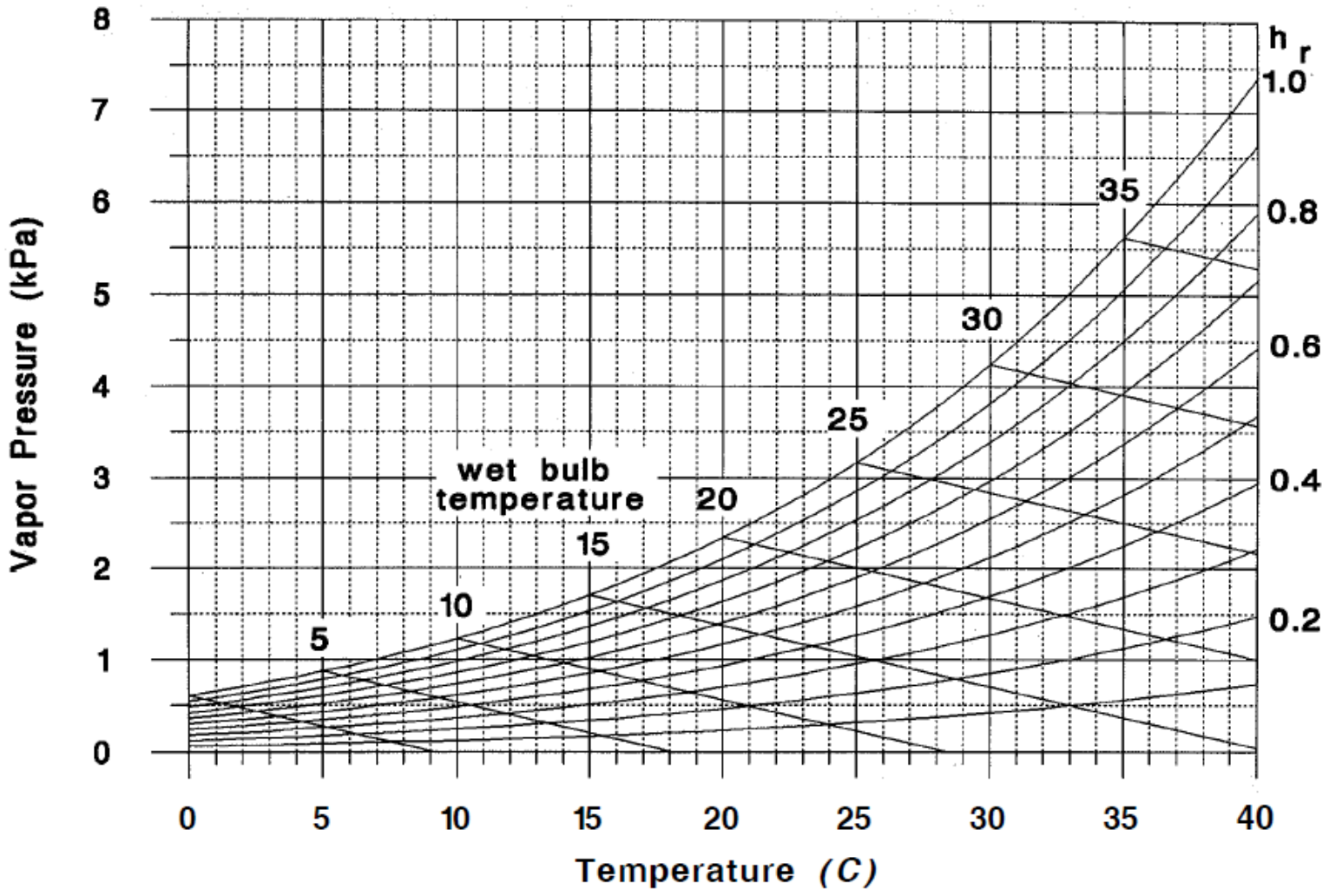

FIGURE 3.2. Vapor pressure-temperature-relative humidity-wet bulb temperature diagram. Wet bulb lines are for sea level pressure.

https://en.wikipedia.org/wiki/Vapour_pressure_of_water

$$e_a = e_s(T_w) - \gamma p_a(T_a - T_w)$$

Partial saturation can be expressed in many ways. Such as mole fraction, relative humidity, vapor deficit, dew point temperature, wet bulb temperature

Show on the graph: VPD, wet bulb temperature

$$\gamma = c_p/\lambda$$

γ: thermodynamic **psychrometer** constant
$C_{p:}$ the specific heat of air (29.3 J mol^{-1} K^{-1})
λ: latent heat of vaporization = 44 kJ mol^{-1}

Spatial and temporal variation

- Diurnal patterns determined by $t°$
- RH and VPD vary with $t°$

- e_a rather stable,
  - Variation minimal, yet:
  - During day - e_a decr. w/ height
  - During night - e_a incr. w/ height

- Because of strong $t°$-dependence, RH itself is a bad parameter,

  Convert to e_a or VPD

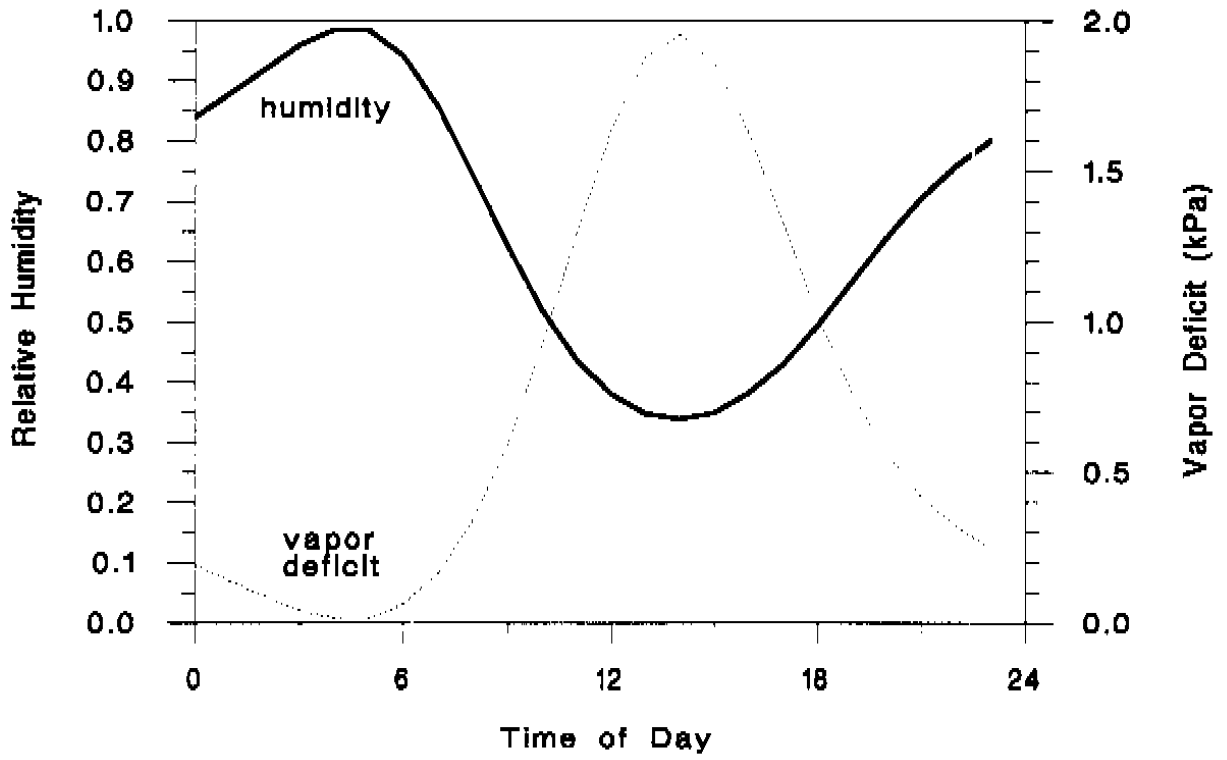

FIGURE 3-3. Diurnal variation in relative humidity and atmospheric vapor deficit for the temperature variation in Fig. 2.2. Vapor pressure is assumed to be constant throughout the day at 1.00 kPa.

Review of Radiation
Solar constant: 1.34-1.36 $kW.m^{-2}$, with about 2% fluctuations
Sun spots: in pairs, ~11 yrs frequency, and from a few days to several months duration
Little ice age (1645-1715)
Greenhouse effects (atmosphere as a selective filter)
Low absorptivity between 8-13 μm
Clouds
Elevated CO_2
Destroy of O_3
O_3 also absorb UV and X-ray

Global radiation budget
Related terms: cloudiness turbidity (visibility), and *albedo*
Lambert's Cosine Law

Other Considerations
Zenith distance (angle)

Other terms
Solar noon: over the meridian of observation
Equinox: the sun passes directly over the equator
Solstice
Solar declination

Path of the Earth around the sun

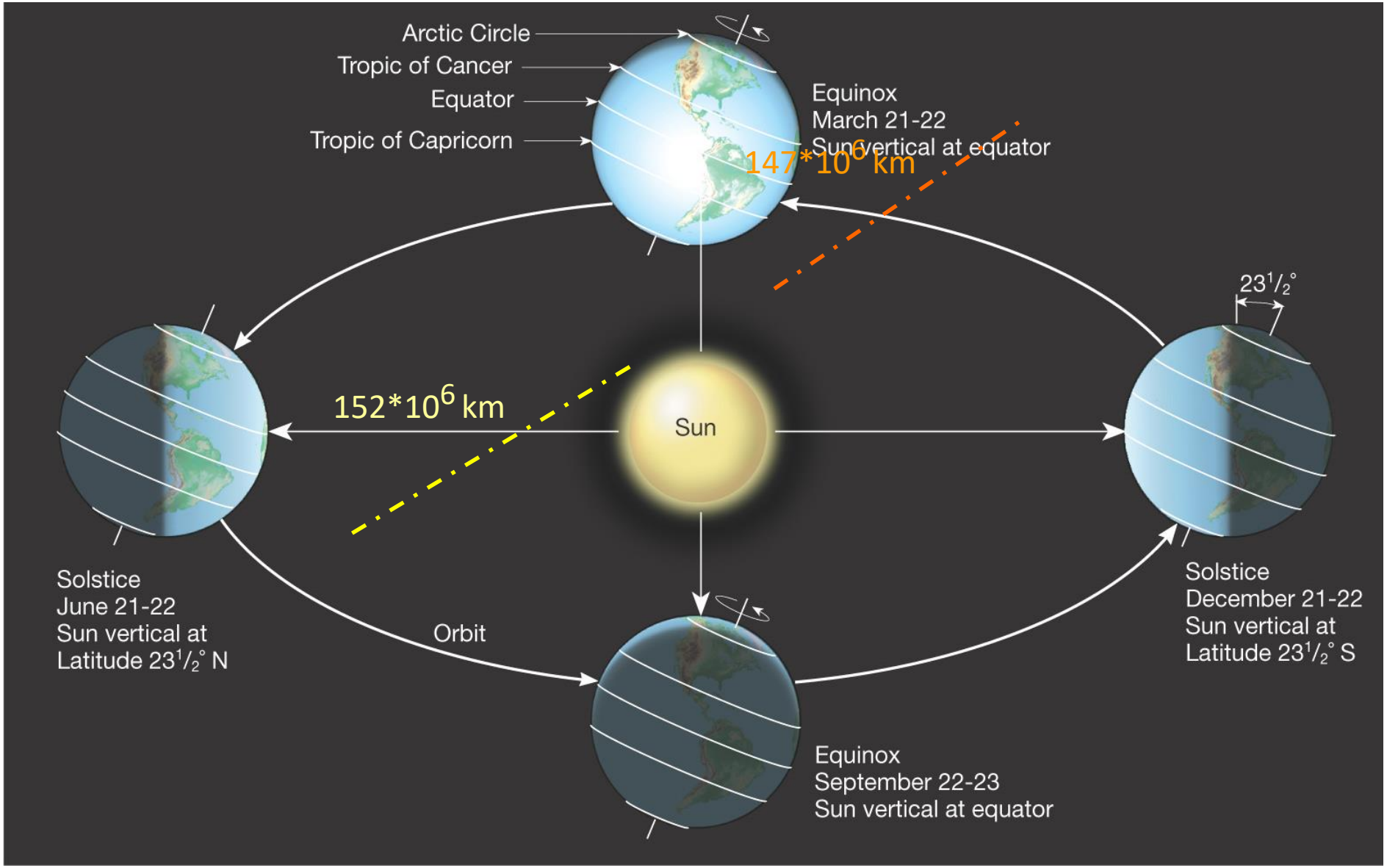

Sun angles and day length

- The location of sun in the sky is described with
  - altitude (β) or zenith angle (ψ)
  - azimuth angle (AZ)
    - $\cos \psi = \sin \beta = \sin\phi \sin\delta + \cos\phi \cos\delta \cos [15(t-t_0)]$
    - $t_0 = 12 - LC - ET$
    - $h_s = \cos^{-1} [(\cos\psi - \sin\phi \sin\delta) / (\cos\phi \cos\delta)]$

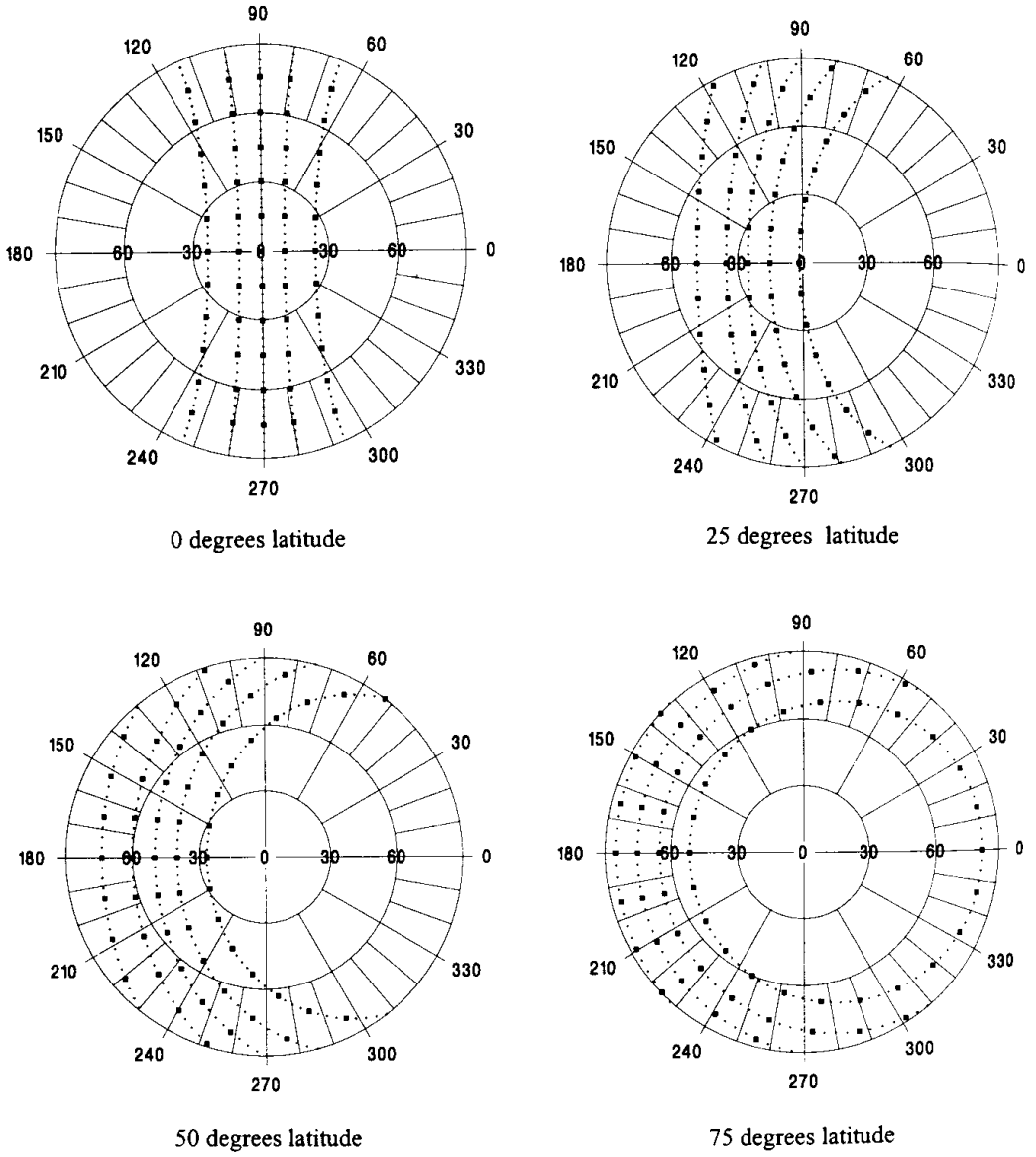

FIGURE 11-1. Sun tracks at declination angles of −23.5, −10, 0, 10, and 23.5° for four different latitudes. Zenith angle grids are the concentric circles. Azimuth angles are shown around the outer circle. North is 0°, east is 90°. Large dots are at one hour time increments.

Radiation

$\mathbf{e = h \bullet c / \lambda}$ Planck's equation

e - energy of photon

h - Planck's constant

c - speed of light

λ - wavelength of radiation

ν - frequency of radiation

$\lambda \bullet \nu = c \rightarrow e = h \bullet \nu$

Blackbody radiation

- Perfect absorber & emitter
- Blackbody absorber in certain wavelength
- SNOW

  poor absorber in 400-700 nm

  black body absorber >5 μm

Stefan-Boltzmann Law

$E = e * \sigma * T^4$

where e is emmisivity (0-1). Blackbody has e of 1,

σ is Stefan-Boltzmann's constant (56.697×10^{-9} W m^{-2} K^{-4})

Spectral distribution of blackbody radiation

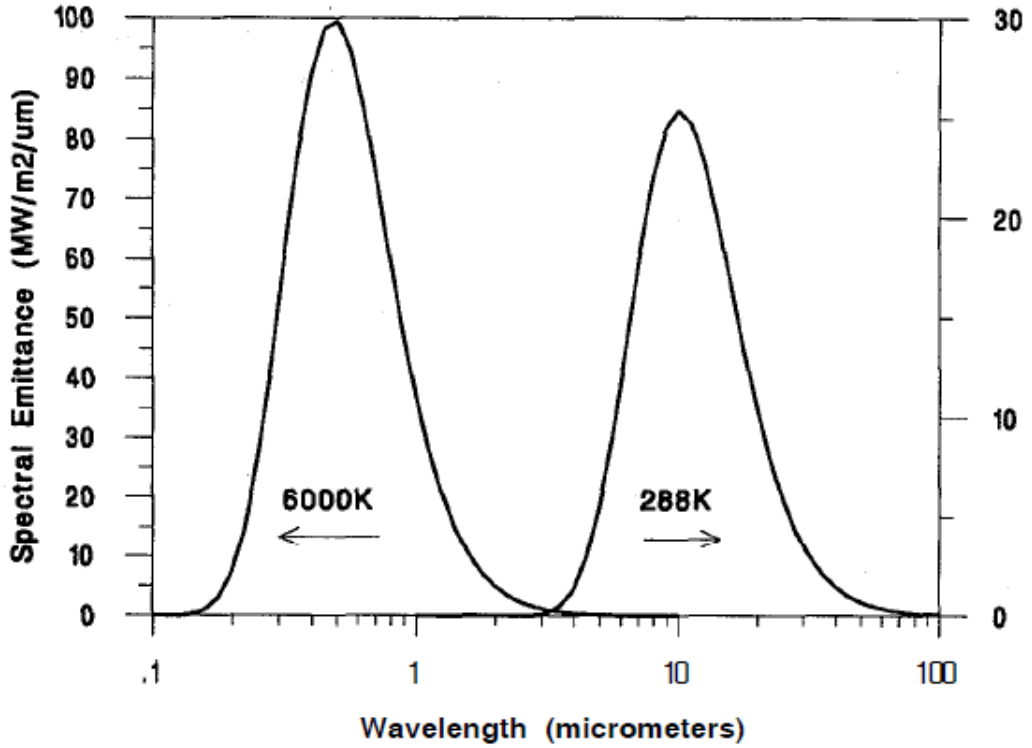

FIGURE 10.4. Emittance spectra for 6000 K and 288 K blackbody sources approximating emission from the sun and the earth.

$$\lambda_m = 2897 \bullet T^{-1}$$

Spectral distribution of solar radiation

PAR – Photosynthetically-active radiation (400-700 um)

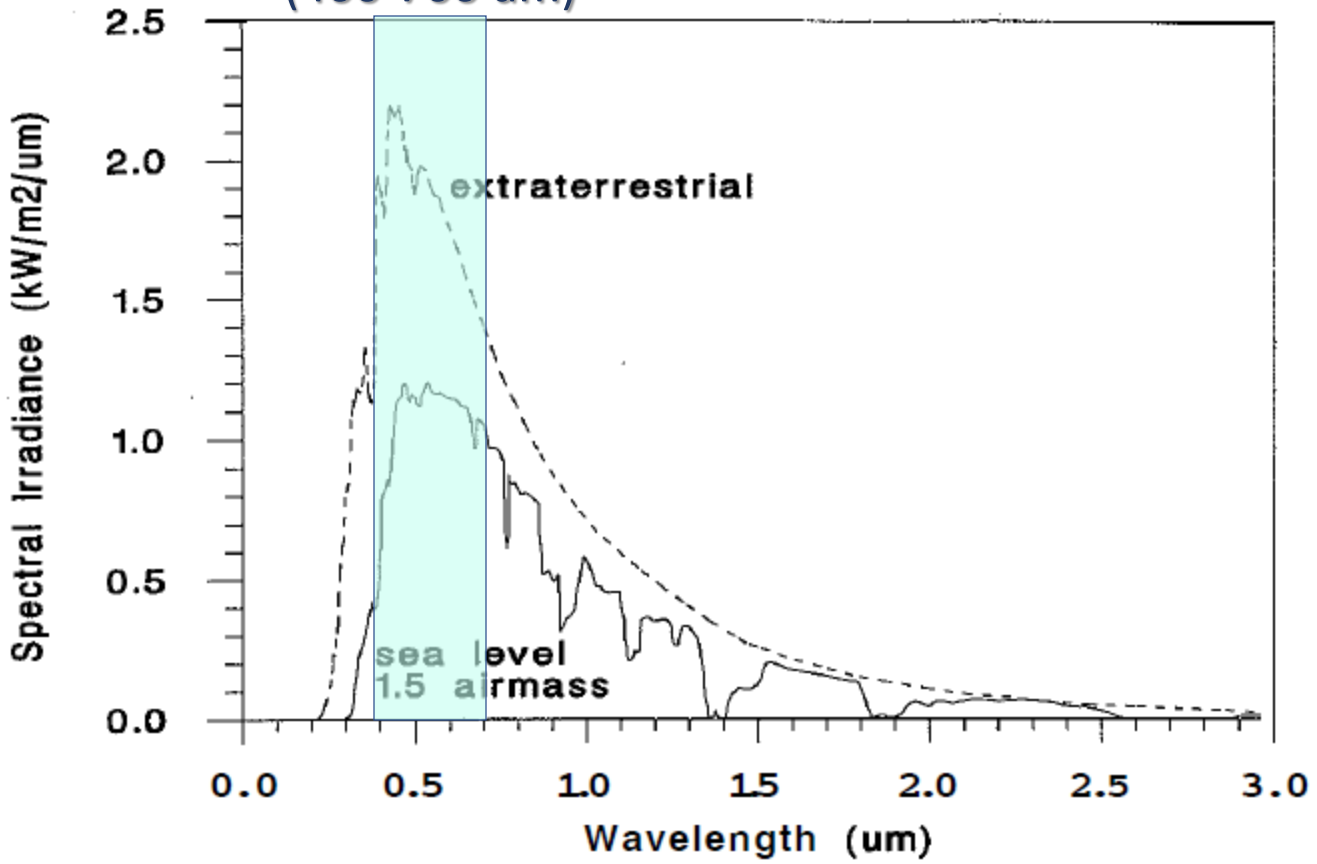

FIGURE 10.5. Spectral irradiance of the sun just outside the atmosphere and at sea level through a 1.5 airmass atmospheric path. Atmospheric absorption at short wavelengths is mainly from ozone. At long wavelengths it is mainly from water vapor (redrawn from Gates, 1980).

Spectral distribution of earth radiation

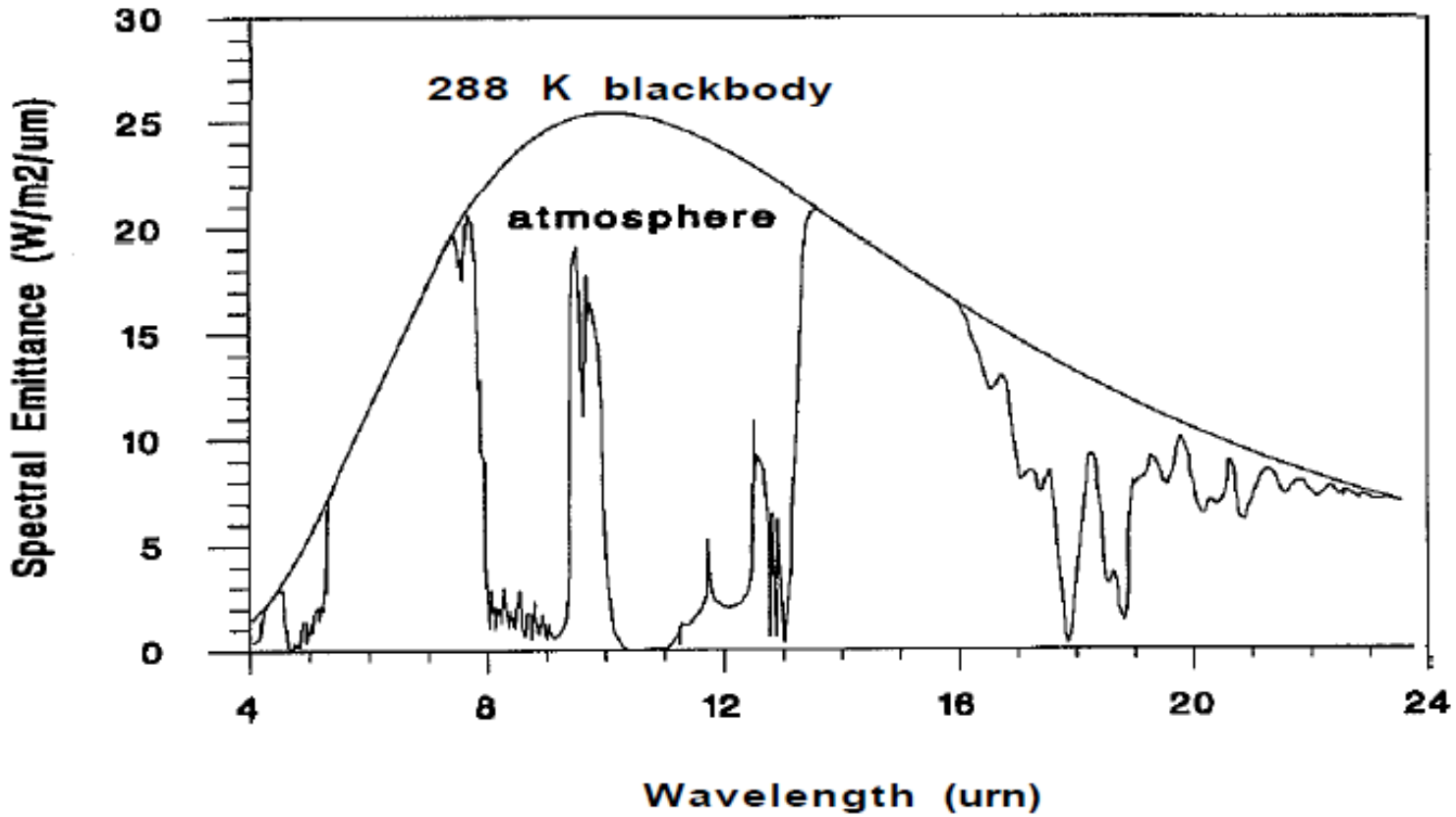

FIGURE 10.6. Spectral distribution of thermal radiation from the earth and from the clear atmosphere. Emission bands below 8 and above 18 μm are mainly from water vapor. Bands between 13 and 18 μm are mainly CO_2. The narrow band at 9.5 μm is from ozone (redrawn from Gates, 1962).

Radiation

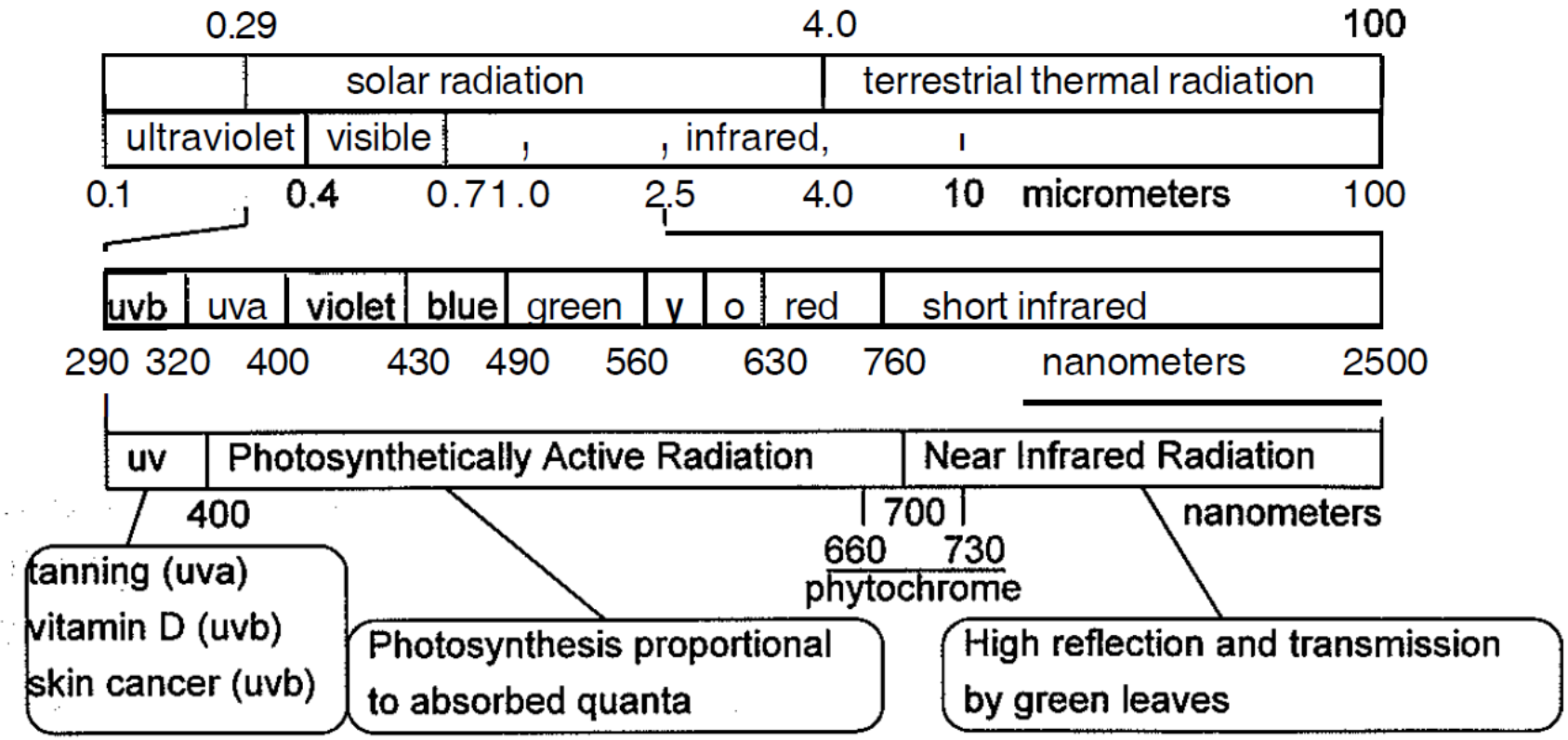

FIGURE 10.1. Part of the electromagnetic spectrum showing names of some of the wavebands and some of the biologically significant interactions with plants and animals.

Definitions and measures

- *Radiant flux* - radiant energy emitted, transmitted or received per unit time
- *Radiant flux density* - radiant flux per unit area
- *Irradiance* - radiant flux density incident on a surface
- *Radiant spectral flux density* - Radiant flux density per unit wavelength interval
- *Radiant intensity* - flux emanating from a surface per unit solid angle
- *Radiance* - radiant flux density emanating from a surface per unit solid angle
- *Spectral radiance* - radiance per unit wavelength interval
- *Radiant emittance* - radiant flux density emitted by a surface

Terminology

- Absorptivity [$\alpha(\lambda)$] - fraction of incident radiant flux at a given wavelength that is absorbed by the material
- Emissivity [$\varepsilon(\lambda)$]
- Reflectivity [$\rho(\lambda)$]
- Transmissivity [$\tau(\lambda)$]

Black body $\alpha(\lambda)=1$, $\rho(\lambda)=\tau(\lambda)=0$

$\varepsilon(\lambda)$: potential emissivity equals to $\alpha(\lambda)$.

Usually ε at longer λ than α because energy loss.

Commonly ε only in infrared range (thermal radiation).

1.4 Solar Radiation

Solar Constant: 1360 - 1380 W m^{-2}

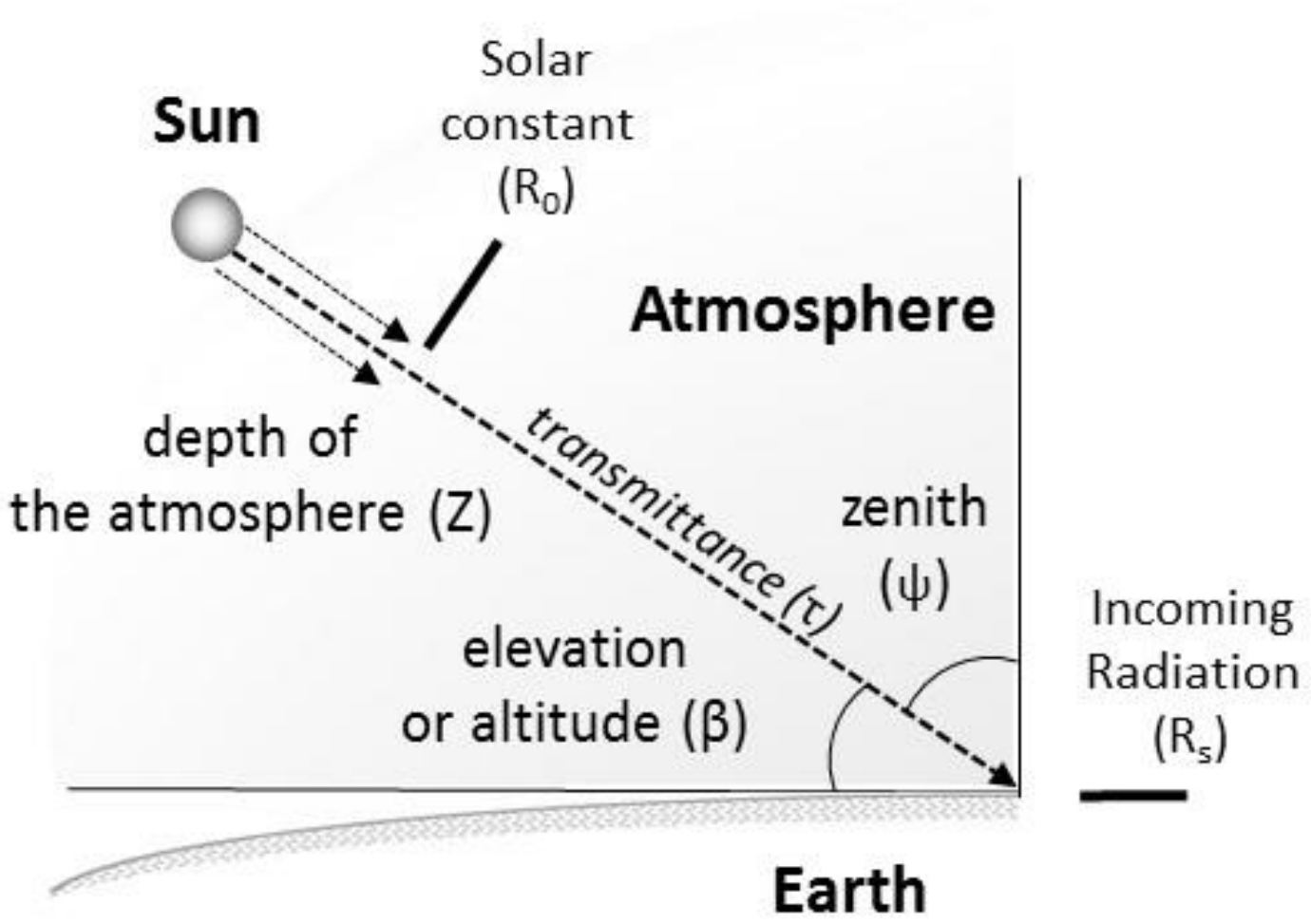

Solar declination (D): an angular distance north (+) or south (-) of the celestial equator of place of the earth's equator.

Solar elevation angle (b): the angular distance from the meridian of the observer (90-θ).

Azimuthal angle: the angle between the true north and the projection of sun's rays onto the horizon.

Turbidity: any condition of the atmosphere which reduced its transparency to radiation, especially to visible radiation.

Albedo: reflection of solar beams (shortwave only)

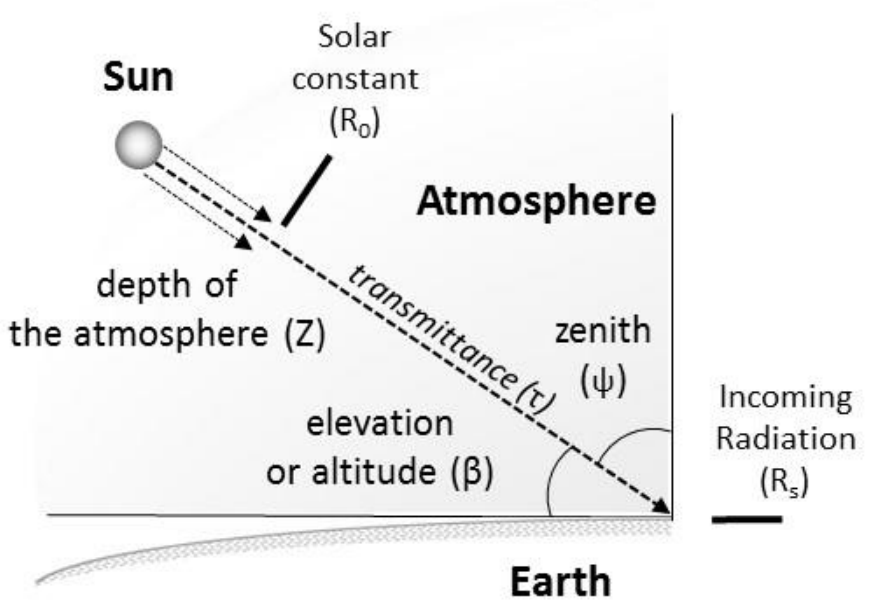

1.4 Solar Radiation

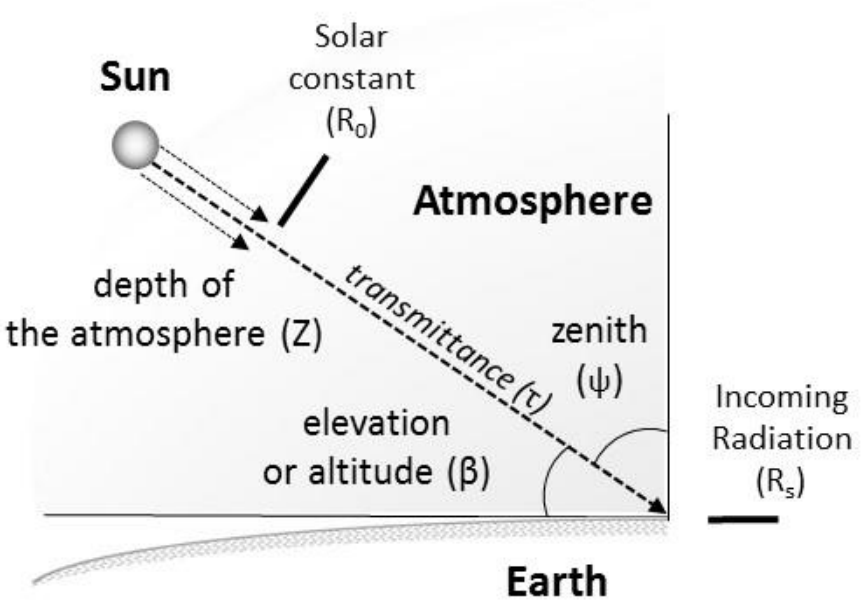

Incoming radiation at land surface:

$$R = \tau \cdot R_0$$

τ is called sky transmittance and varies with the path length of solar beams through the atmosphere and air turbidity.

R can be modeled with Beer's law

$$R = R_0 \cdot e^{-k \cdot z}$$

where *k* is the atmospheric extinction coefficient (km^{-1}) and *z* (km) is the path length through the atmosphere, which depends on the solar elevation (β,degree) and solar declination (τ).

The horizontal flux density of solar radiation at the land surface is calculated with cosine law

$$R_s = R \cdot \cos(\psi)$$

where ψ is zenith angle (degree) ($\psi = 90 - \beta$).

Lambert's cosine law

$\Phi = \Phi_0 \bullet \cos\theta$

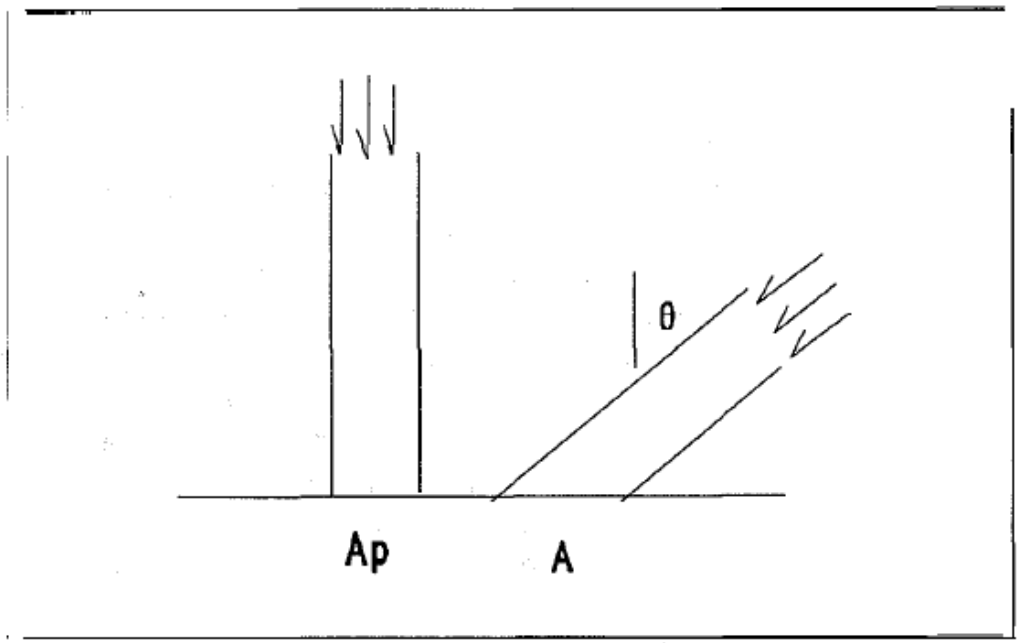

FIGURE 10.3. The area covered by a beam of parallel light increases as the angle θ between the beam and a normal to the surface increases.

Lambertian surface: ideal diffusely reflecting surface

$\rho(\lambda) = a \bullet \cos\lambda$

Beer-Lambert's Law

$$I = I_0 e^{-k * b}$$

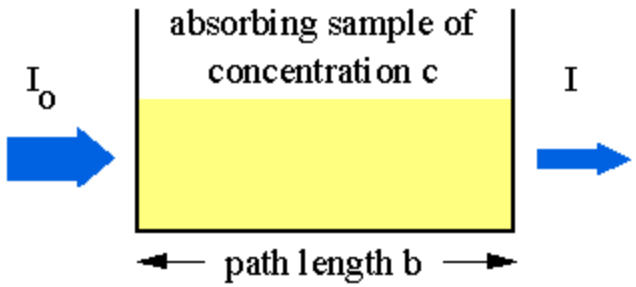

- Attenuation of radiation in a homogeneous medium
- Applies for wavebands narrow enough where ***k*** remains constant.

Hemispherical photos and applications: A "standard" method to characterize light environments beneath forest canopies

Radiation Balance Model

Albedo = R_e: R_t

Tables S1 Summary table for the overall linear (downscaling) models at Eq. (1) for the growing season (GS) and monthly α_{SHO} (dependent variable) across the entire Kalamazoo River watershed.

	variable	estimates	SE	t	p	DF	adj. R^2
GS	barren	0.152	0.000	1340.300	***	9	0.995
	cropland	0.174	0.000	26281.727	***		
	forest	0.145	0.000	13171.109	***		
	grassland	0.129	0.000	1347.355	***		
	pasture	0.165	0.000	5715.941	***		
	shrubland	0.138	0.000	653.438	***		
	urban	0.145	0.000	10926.929	***		
	water	0.091	0.000	2815.767	***		
	wetland	0.154	0.000	12248.465	***		
monthly	barren	0.237	0.003	93.220	***	9	0.745
	cropland	0.283	0.000	1904.740	***		
	forest	0.185	0.000	745.962	***		
	grassland	0.171	0.002	76.378	***		
	pasture	0.260	0.001	398.528	***		
	shrubland	0.149	0.005	32.996	***		
	urban	0.215	0.000	715.211	***		
	water	0.183	0.001	251.948	***		
	wetland	0.215	0.000	756.229	***		

Signif. codes: “***” p-value < 0.001, “**” p-value < 0.01, “*” p-value < 0.05, “·” p-value < 0.1, “ ” p-value > 0.1.

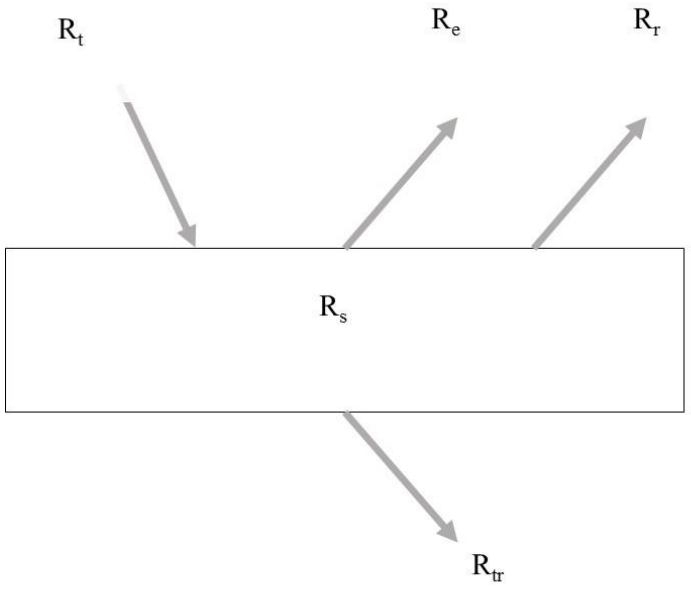

Diel change of short-wave radiation in and under forest canopies (Chen et al. 1999)

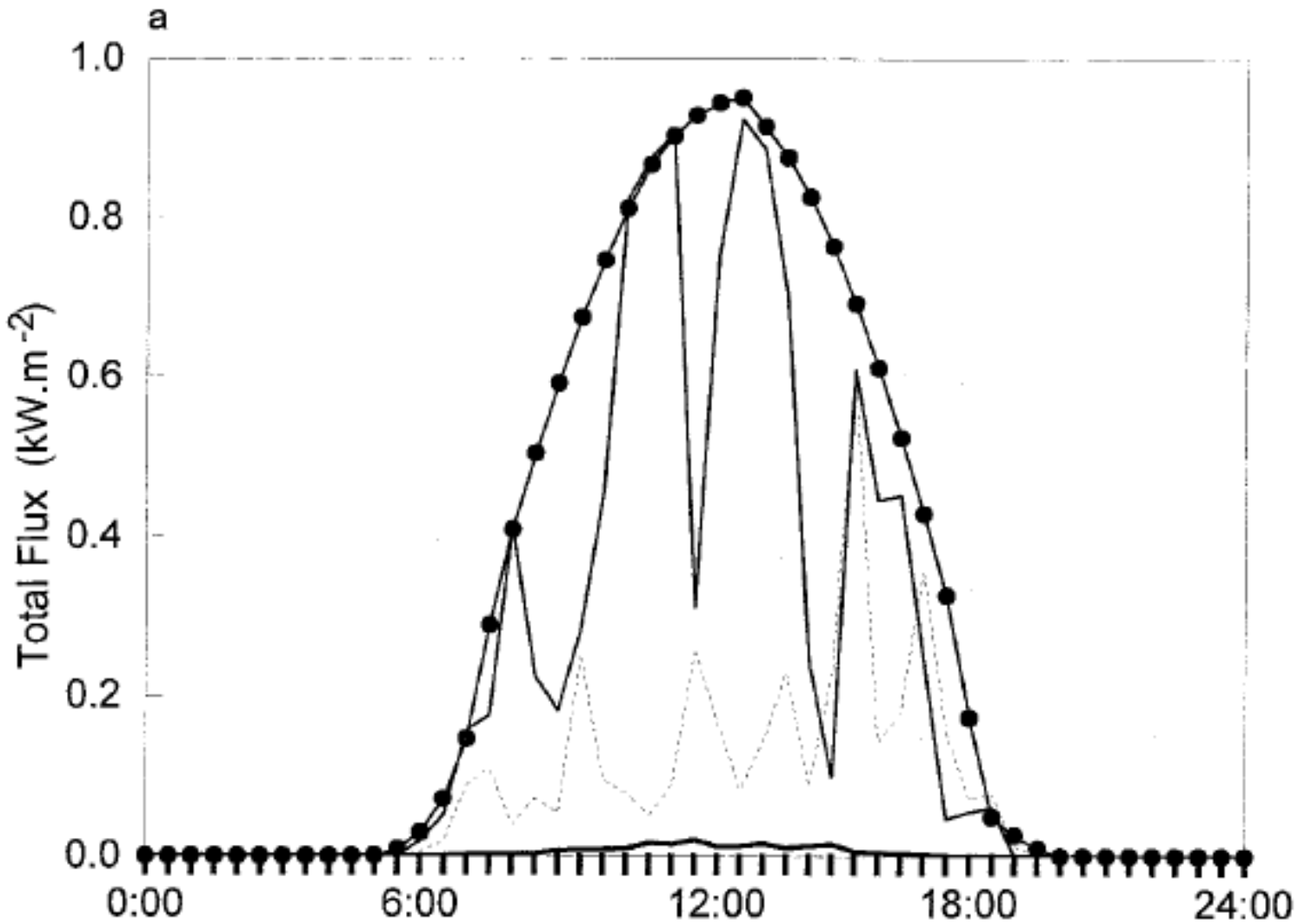

Direct and diffuse shortwave irradiance

- S_p - direct irradiance perpendicular to the beam
- S_d - diffuse sky irradiance on a horizontal plane
- S_r - reflected radiation from the ground
- S_b - beam irradiance on a horizontal plane
- S_t - total irradiance on a horizontal plane (global irradiance = $S_b + S_d$)

$$S_b = S_p \cos \psi$$

$$S_p = S_{p0} t^m$$

$t \approx 0.7$ (0.45...0.75) clear

$t < 0.4$ overcast

TABLE 11.2. Shortwave reflectivity (albedo) of soils and vegetation canopies.

Surface	Reflectivity	Surface	Reflectivity
Grass	0.24–0.26	Snow, fresh	0.75–0.95
Wheat	0.16–0.26	Snow, old	0.40–0.70
Maize	0.18–0.22	Soil, wet dark	0.08
Beets	0.18	Soil, dry dark	0.13
Potato	0.19	Soil, wet light	0.10
Deciduous forest	0.10–0.20	Soil, dry light	0.18
Coniferous forest	0.05–0.15	Sand, dry white	0.35
Tundra	0.15-0.20	Road, blacktop	0.14
Steppe	0.20	Urban area (average)	0.15

Radiation under clouds

$$S_d = S_t$$

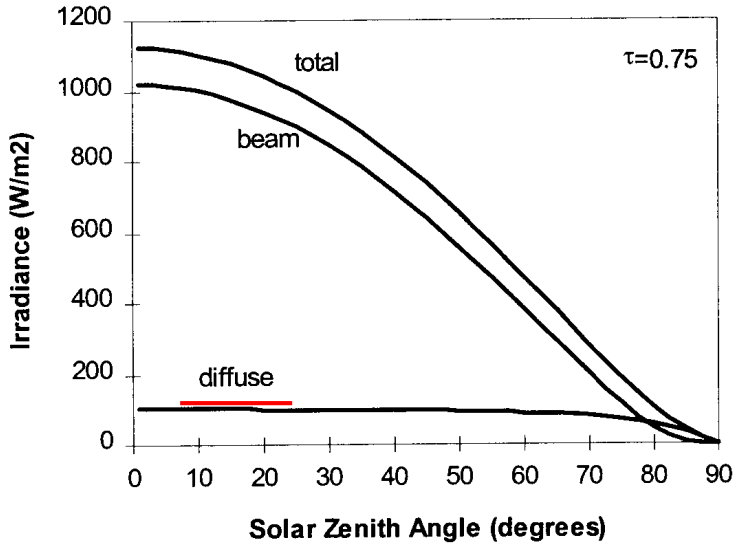

FIGURE 11.2. Beam (S_b), diffuse (S_d), and total solar radiation (S_t) as a function of zenith angle for a very clear sky.

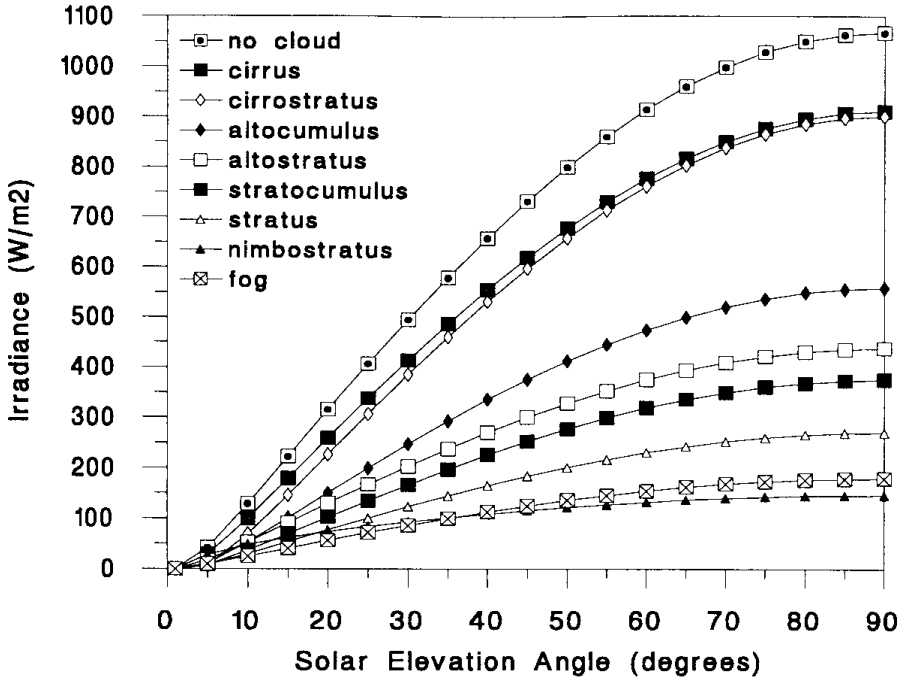

FIGURE 11.4. Solar irradiance under cloud cover for various cloud types and solar elevation angles (data from List, 1971).

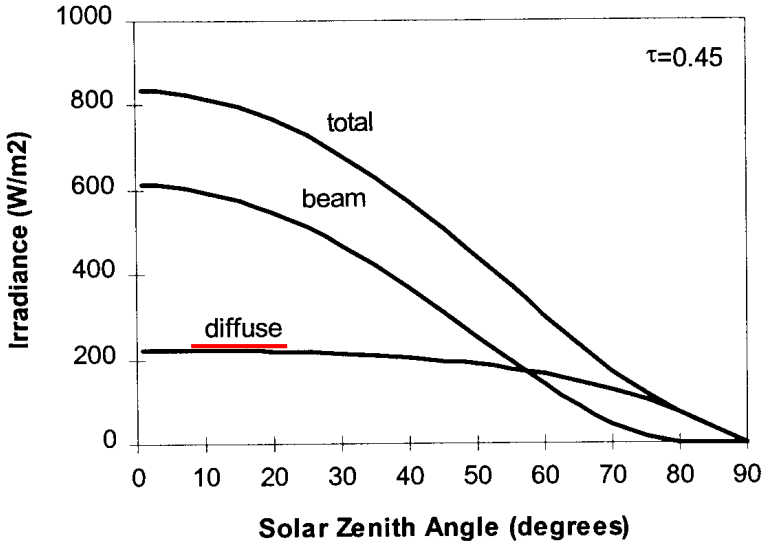

FIGURE 11.3. Similar to Fig. 11.2, but for turbid or polluted air.

Figure 1-5. (a) Diurnal change of solar zenith angle (degree) for the 22nd day of June-December in 2016 at the KBS-switchgrass site; (b) simulated incoming solar radiation (R_s, W m^{-2}) by assuming a transmittance of 0.85 on June 22 and a monthly decreasing rate of 4% for the seven days during June-December based on Eqs. 1.17 – 1.19; and (c) the simulated/measured R_s values for September 22, 2016, by assuming ±10% and ±20% variation of sky transmittance from the mean value (*i.e.*, 0.75) used in (b).
Figure 1-5

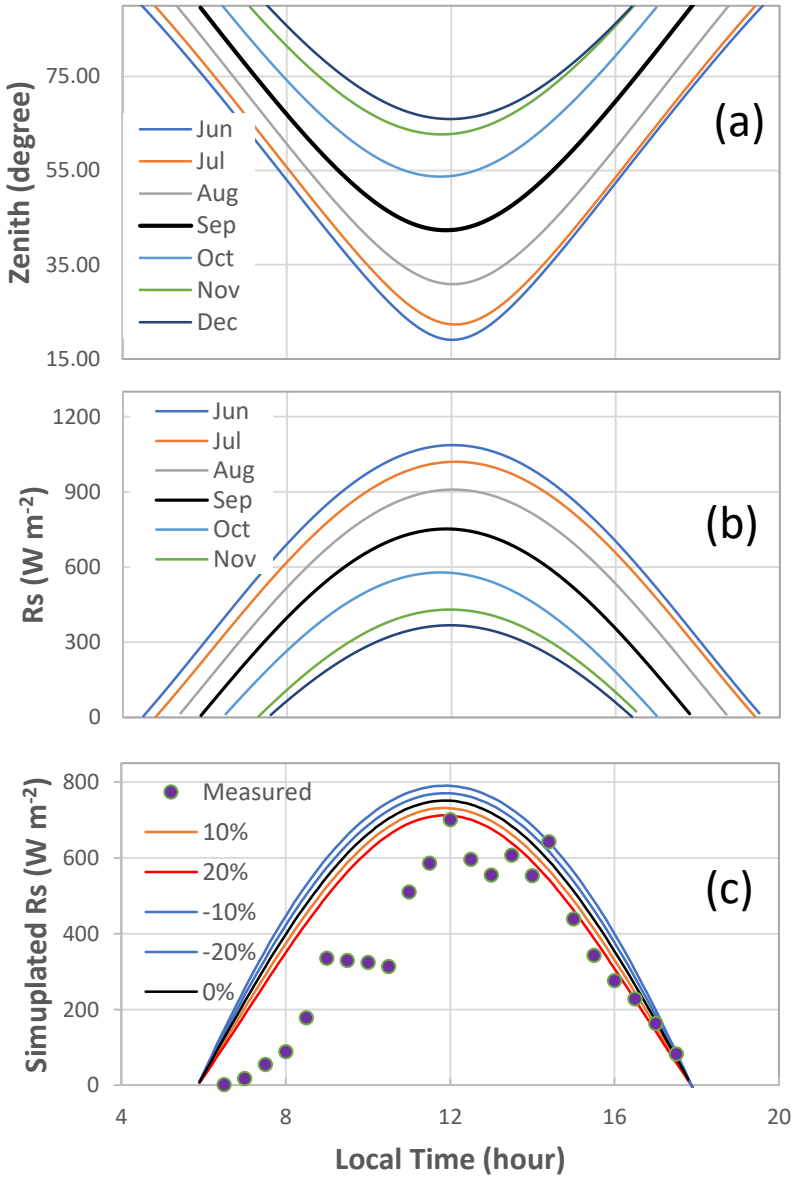

Demo of the solar.PY model (S1-4)

1.5 Heat Storages in Soil, Air and Vegetation

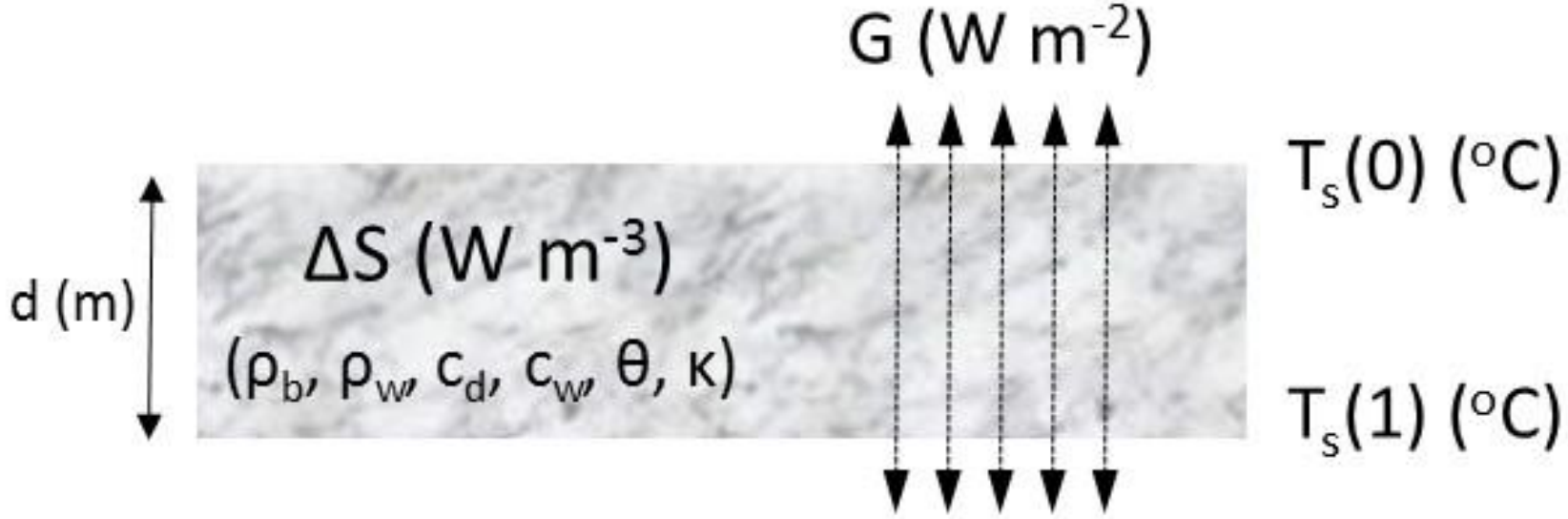

Figure 1-6. Schematic illustration of heat flow through, and storage in, a thin plate (*e.g.*, topsoil layer), labeled as *G* and *ΔS*, respectively. Temperature difference on the two sides of the plate and soil properties jointly determined the magnitude and dynamics of *G* and *ΔS*, including thermal conductivity (κ), density, water content (ϑ) and specific heat capacity of the soil.

1.5 Heat Storages in Soil, Air and Vegetation

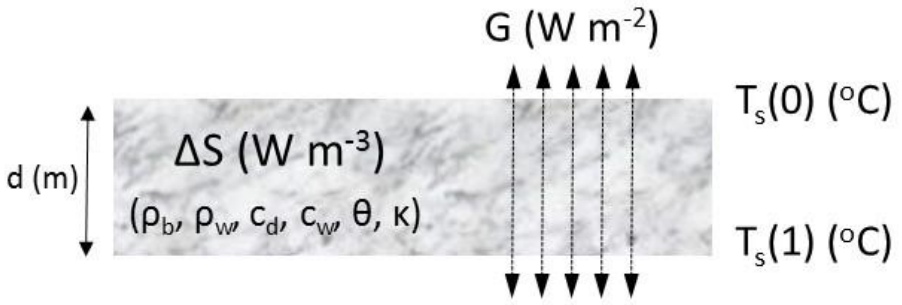

The heat flux density (G, W m^{-2}) is calculated as:

$$G = \kappa \cdot \frac{\Delta T}{d}$$

where κ (W m^{-1} K^{-1}) is the thermal conductivity of the soil and d (m) is the thickness of the soil layer.

The heat storage (ΔS, W m^{-3}) over a period of time (t) can be calculated as

$$\Delta S = (\rho_b.c_b + \theta \cdot \rho_w \cdot c_w)\frac{\Delta T}{\Delta t} \cdot d$$

where ρ_b (kg m^{-1}) is the soil bulk density, ρ_w is the density of water, c_d (890 J kg^{-1} K^{-1}) and c_w (4190 J kg^{-1} K^{-1}) are the specific heat capacities of the dry mineral soil and the soil water, respectively, θ is the volumetric soil water content (%), and $\Delta T/\Delta t$ (K s^{-1}) is the mean soil temperature change at the time t interval (*i.e.*, can be approximated with the mean values of $T_s(0)$ and $T_s(1)$ at a given time).

Ecological Applications, 27(2), 2017, pp. 485–502

Grazing effects on surface energy fluxes in a desert steppe on the Mongolian Plateau

Changliang Shao,[1,4] Jiquan Chen,[1] Linghao Li,[2] Gang Dong,[3] Juanjuan Han,[2] Michael Abraha,[1] and Ranjeet John[1]

- G can be as high as 50-100 W m^{-2} in an arid ecosystem (e.g., Desert);
- It is about 5-20 W m^{-2} in temperate forests

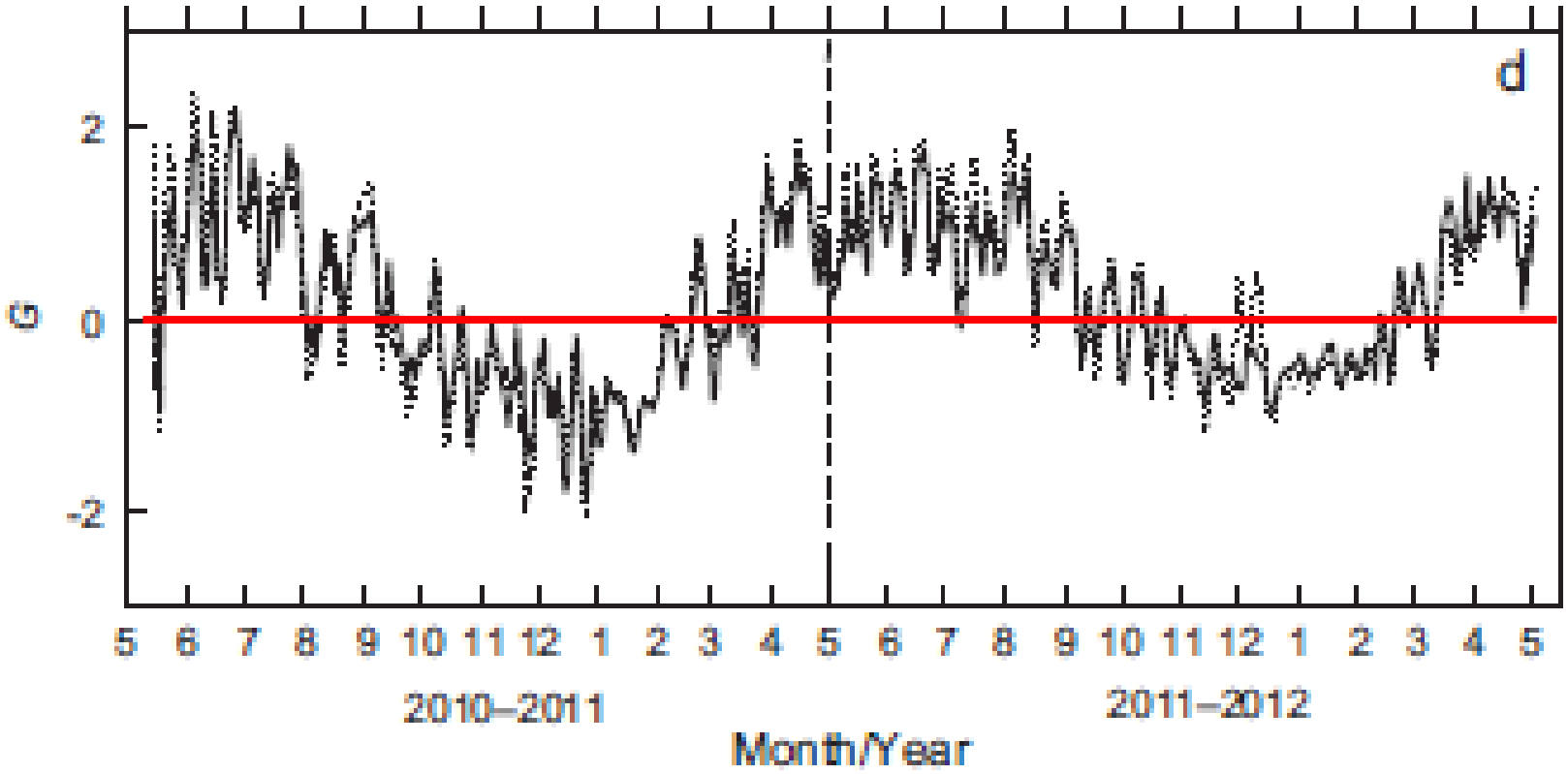

1.6 Vertical Profile of Wind Speed

Terminology

- Mechanical turbulence
- Thermal turbulence

Causes

- Wind at higher altitude
- Horizontal temperature/density
- Topographic variation (e.g., cold air drainage)
- Movement of objects
- Instability of atmosphere

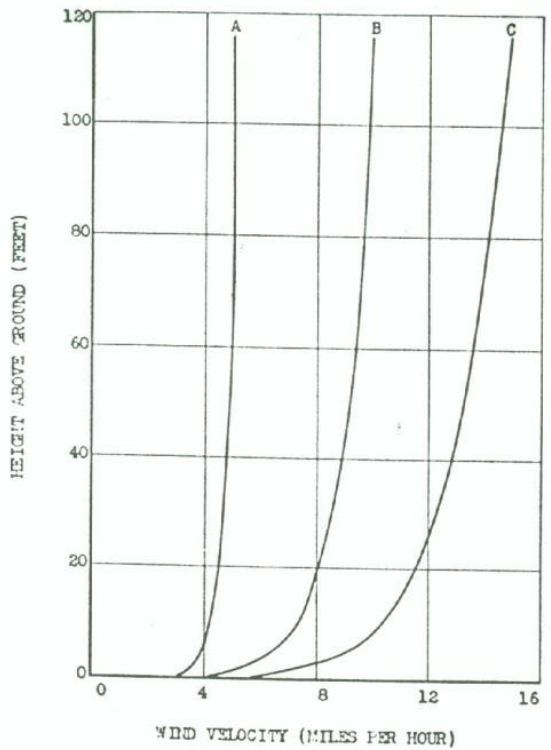

Fig. 3.—Grassland site: Distribution of wind velocities with height for wind velocities of 5 (A), 10 (B), and 15 (C) miles per hour measured 116 feet above the ground.

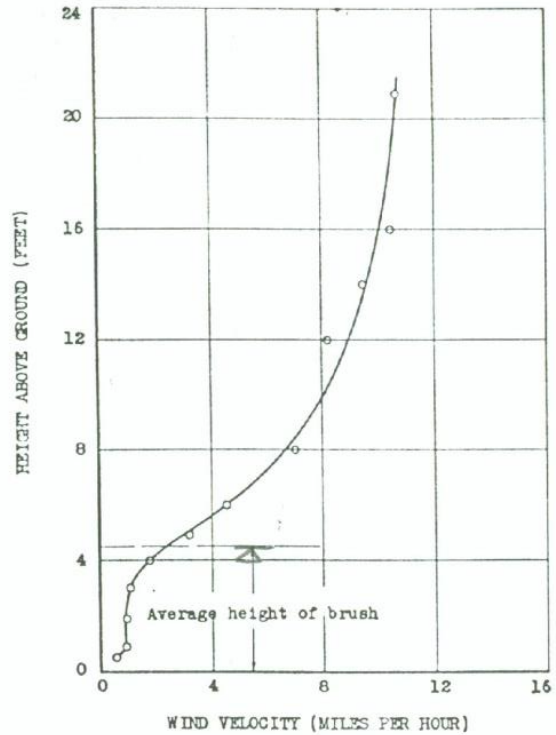

Fig. 5.—Brush site: Distribution of wind velocities near the ground with an average velocity of 10.7 miles per hour measured 21 feet above the ground.

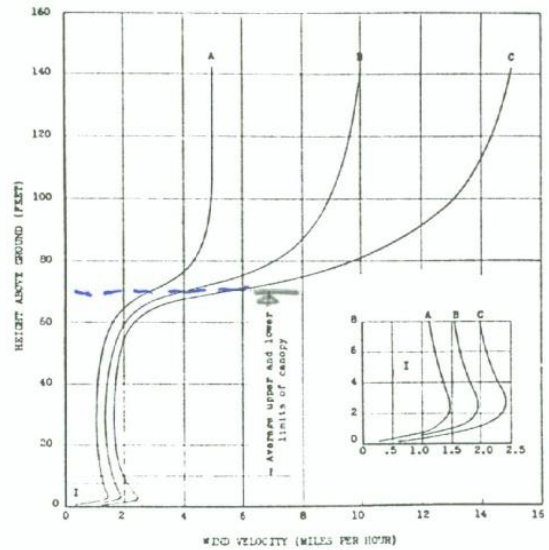

Fig. 4.—Ponderosa pine site: Distribution of wind velocities with height as affected by the timber canopy for wind velocities of 5 (A), 10 (B), and 15 (C) miles per hour measured 142 feet above the ground.

Wind Direction & Windroses

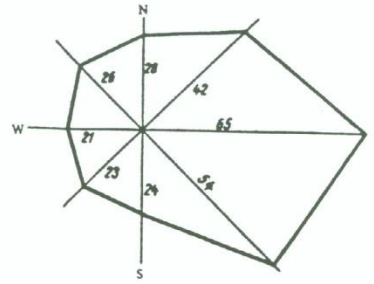

FIGURE 109. Wind rose

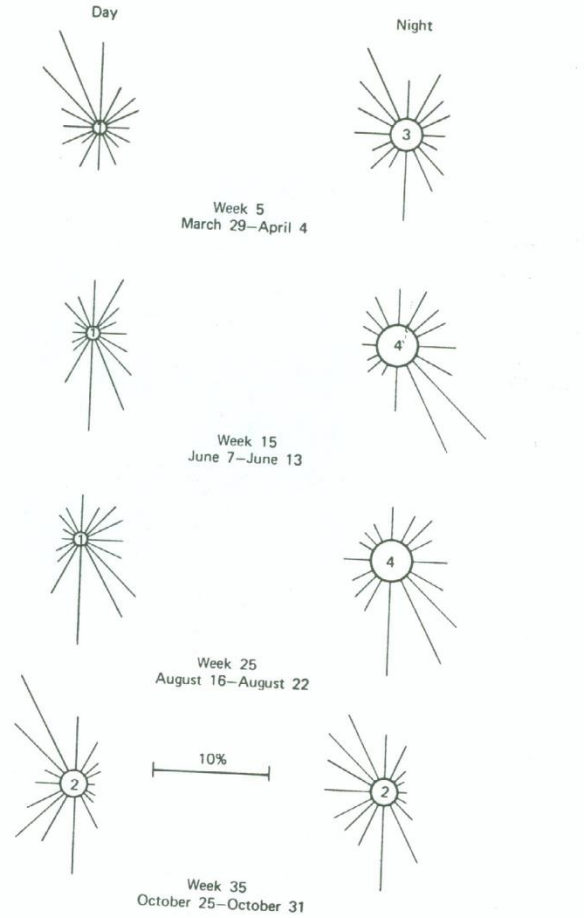

Fig. 4.10 Percentage frequencies of wind direction for day and night during 4 weeks of the growing season at Grand Island, Nebraska. Percent of calm hours indicated in center circle (after Rosenberg, 1965).

1.6 Vertical Profile of Wind Speed

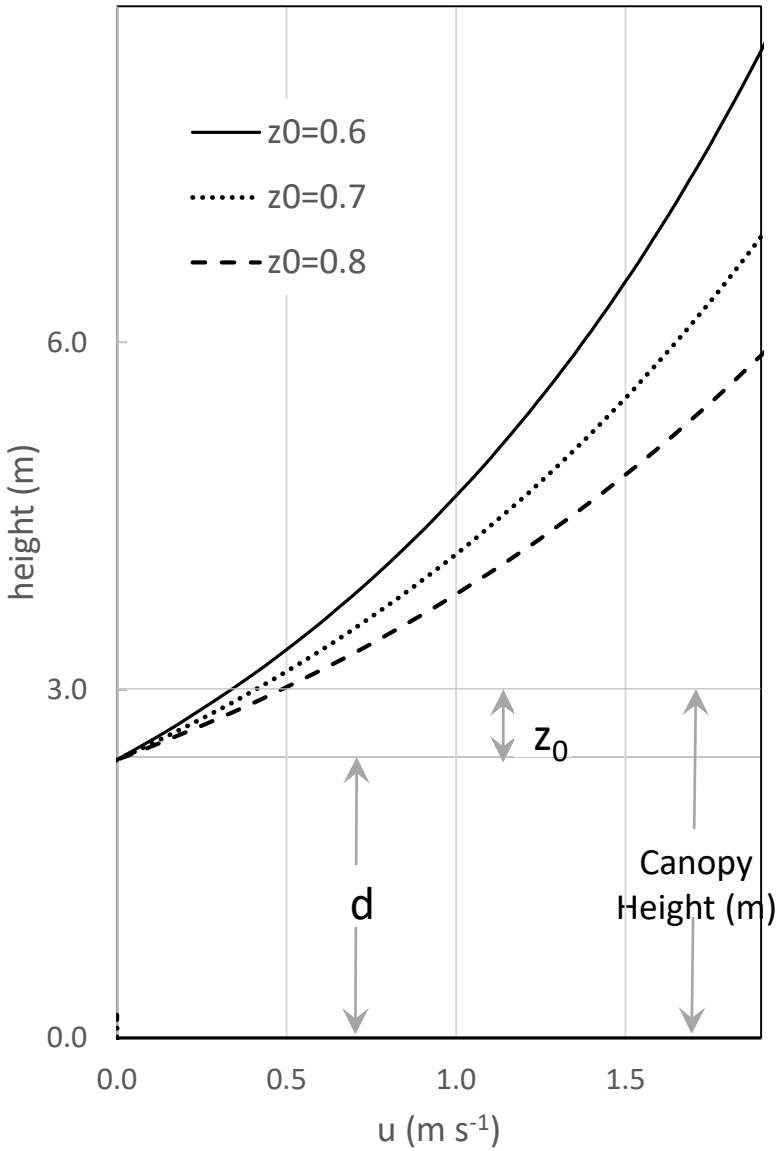

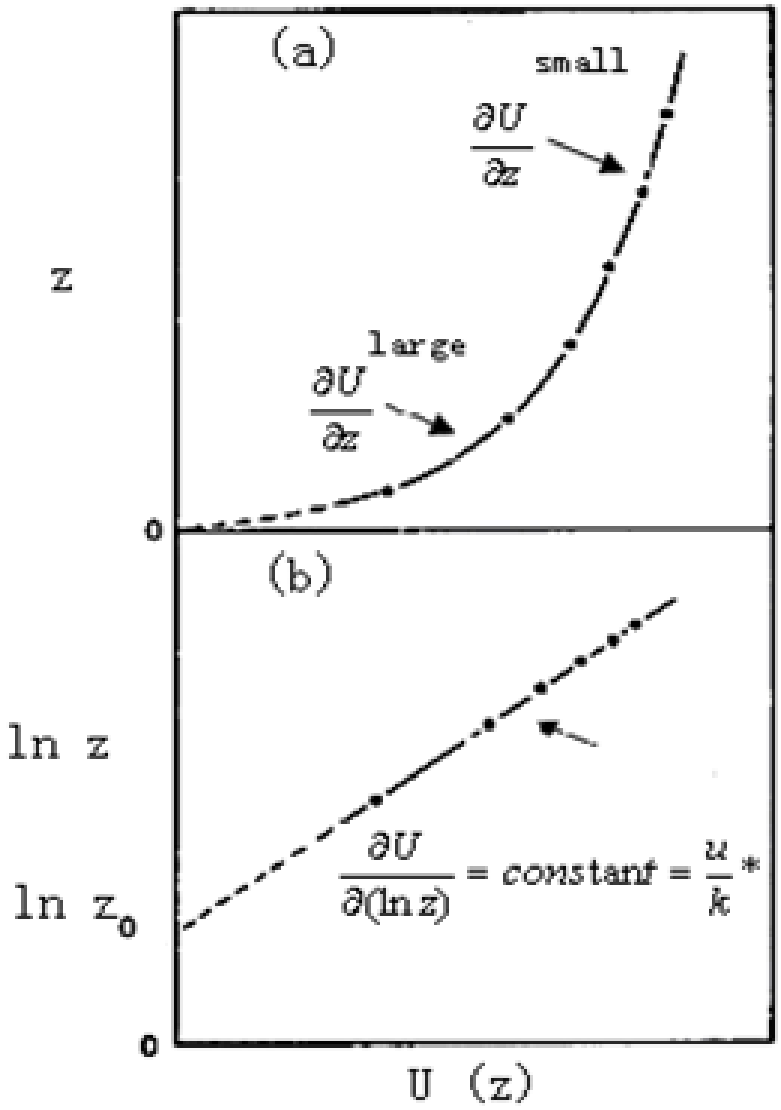

Typical wind profile over an open, level (relatively smooth) site: (a) plotted linearly against height z; (b) plotted against the logarithm of z.

Typical wind profile over uniform level vegetation of height h: (a) plotted linearly against z; (b) plotted against the logarithm of distance above the zero plane displacement level.

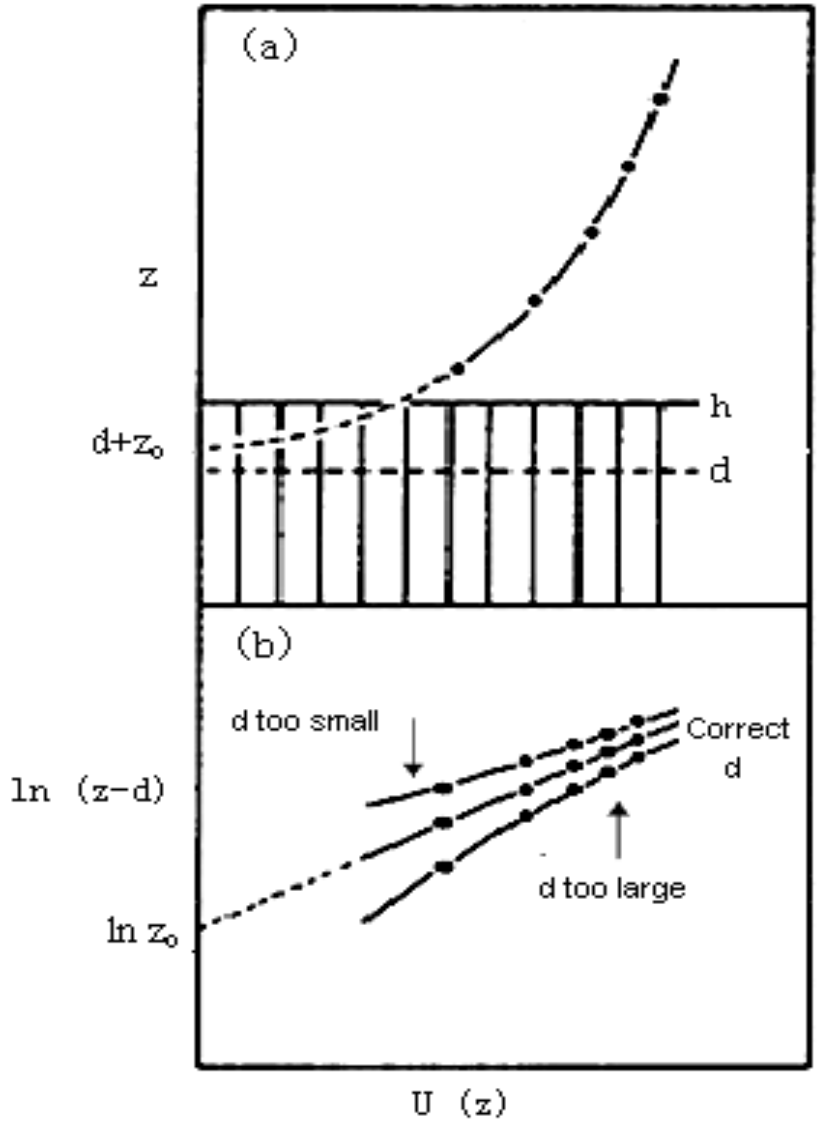

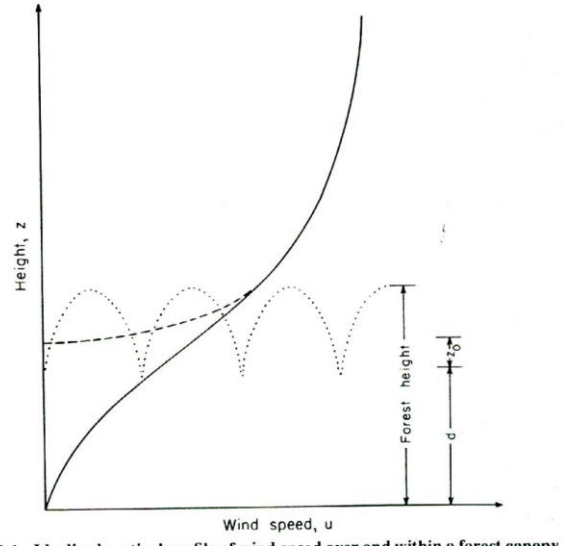

Fig. 4.1. Idealized vertical profile of wind speed over and within a forest canopy.

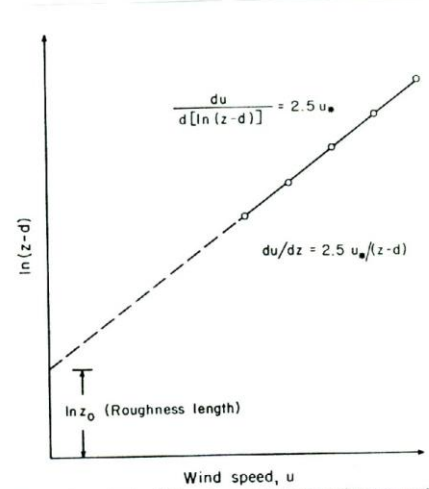

Fig. 4.2. Graphical analysis of the observed wind profile over a forest canopy under neutral conditions.

Wind profiles

Vertical profiles of winds can be described using a logarithm function:

$$U(z) = \frac{u^*}{\kappa} \ln\left(\frac{z}{z_m}\right)$$

Where

U: horizontal wind speed ($m.s^{-1}$)

Z: height (m) above the ground

u*: friction velocity ($m.s^{-1}$) which is related to shearing stress (τ) and air density (ρ), or

See S1-4 on simulating vertical wind profile

$$u* = \left(\frac{\tau}{\rho}\right)^{1/2}$$

κ: von Karmon's constant (≈ 0.4)

Z_m: surface roughness or roughness length (m)

The change of U with z is:

$$\frac{\partial(U)}{\partial(\ln[z / z_m])} = \frac{u*}{\kappa}$$

For wind profiles through vegetation, a zero plane displacement (d) is required (i.e., to shit the curve upward):

$$U(z) = \frac{u^*}{\kappa} \ln\left(\frac{z - d}{z_m}\right)$$

Questions